

## Chemical loss of ozone during the Arctic winter of 1999/2000: An analysis based on balloon-borne observations

R. J. Salawitch,<sup>1</sup> J. J. Margitan,<sup>1</sup> B. Sen,<sup>1</sup> G. C. Toon,<sup>1</sup> G. B. Osterman,<sup>1</sup> M. Rex,<sup>2</sup>  
J. W. Elkins,<sup>3</sup> E. A. Ray,<sup>3,4,5</sup> F. L. Moore,<sup>3,4</sup> D. F. Hurst,<sup>3,4</sup> P. A. Romashkin,<sup>3,4</sup>  
R. M. Bevilacqua,<sup>6</sup> K. W. Hoppel,<sup>6</sup> E. C. Richard,<sup>4,5</sup> and T. P. Bui<sup>7</sup>

Received 9 March 2001; revised 24 August 2001; accepted 24 August 2001; published 11 September 2002.

[1] Simultaneous balloon-borne observations of ozone ( $O_3$ ) and nitrous oxide ( $N_2O$ ), a long-lived tracer of dynamical motion, are used to quantify the chemical loss of ozone in the Arctic vortex during the winter of 1999/2000. Chemical loss of ozone occurred between altitudes of about 14 and 22 km (pressures from  $\sim 120$  to 30 mbar) and resulted in a  $61 \pm 13$  Dobson unit reduction in total column ozone between late November 1999 and 5 March 2000 (the date of the last balloon-borne measurement considered here). This loss estimate is valid for the core of the vortex during the time period covered by the observations. It is shown that the observed changes in the  $O_3$  versus  $N_2O$  relation were almost entirely due to chemistry and could not have been caused by dynamics. The chemical loss of column ozone inferred from the balloon-borne measurements using the “ozone versus tracer” technique is shown to compare well with estimates of chemical loss found using both the Match technique (as applied to independent ozonesonde data) and the “vortex-averaged descent” technique (as applied to Polar Ozone and Aerosol Measurement (POAM) III satellite measurements of ozone). This comparison establishes the validity of each approach for estimating chemical loss of column ozone for the Arctic winter of 1999/2000. *INDEX TERMS*: 0340 Atmospheric Composition and Structure: Middle atmosphere—composition and chemistry; 0341 Atmospheric Composition and Structure: Middle atmosphere—constituent transport and chemistry (3334); 9315 Information Related to Geographic Region: Arctic region; *KEYWORDS*: ozone depletion, Arctic ozone loss

**Citation:** Salawitch, R. J., et al., Chemical loss of ozone during the Arctic winter of 1999/2000: An analysis based on balloon-borne observations, *J. Geophys. Res.*, 107(D20), 8269, doi:10.1029/2001JD000620, 2002.

### 1. Introduction

[2] The SAGE III Ozone Loss and Validation Experiment (SOLVE) and Third European Stratospheric Experiment on Ozone (THESEO 2000) collaborative field campaign during the winter of 1999/2000 was designed to improve our understanding of the effects of human activity on the abundance of Arctic ozone. During Arctic winter, the total column abundance of  $O_3$  within the vortex circulation system is often essentially constant with time, reflecting a balance of dynamical supply of ozone to high-latitudes and chemical loss within the vortex fueled by halogens that are

largely derived from anthropogenic sources [e.g., *Chipperfield and Jones*, 1999]. The Arctic winter of 1999/2000 was characterized by temperatures cold enough to allow formation of polar stratospheric clouds (PSCs) over widespread regions [e.g., *Manney and Sabutis*, 2000; *Bevilacqua et al.*, 2002], leading to highly elevated levels of ClO [e.g., *Santee et al.*, 2000; *Vömel et al.*, 2001] and large amounts of chemical loss of ozone [e.g., *Sinnhuber et al.*, 2000; *Hoppel et al.*, 2002; *Richard et al.*, 2001; *Rex et al.*, 2002; *Schoeberl et al.*, 2002]. A comprehensive description of Arctic ozone and the ability to estimate its future evolution require a quantitative understanding of both chemical and dynamical processes that affect ozone [e.g., *Shindell et al.*, 1998]. Our study primarily focuses on the quantification of the chemical loss of Arctic ozone that occurred throughout the stratospheric column during the winter of 1999/2000.

[3] Three primary measurement techniques have been used to quantify the chemical loss of Arctic  $O_3$  during the winter of 1999/2000. The first method, termed the “ozone versus tracer” technique, involves simultaneous measurements of  $O_3$  and long-lived gases such as  $N_2O$  or  $CH_4$  that act as tracers of dynamical motion. This technique has been used to define chemical loss for past Arctic winters based on in situ measurements near 20 km [e.g., *Proffitt et al.*, 1990, 1993] and satellite measurements from the Halogen Occul-

<sup>1</sup>Jet Propulsion Laboratory, California Institute of Technology, Pasadena, California, USA.

<sup>2</sup>Alfred Wegener Institute for Polar and Marine Research, Potsdam, Germany.

<sup>3</sup>National Oceanic and Atmospheric Administration Climate Monitoring and Diagnostics Laboratory, Boulder, Colorado, USA.

<sup>4</sup>Cooperative Institute for Research in Environmental Sciences, University of Colorado, Boulder, Colorado, USA.

<sup>5</sup>National Oceanic and Atmospheric Administration Aeronomy Laboratory, Boulder, Colorado, USA.

<sup>6</sup>Naval Research Laboratory, Washington, D.C., USA.

<sup>7</sup>NASA Ames Research Center, Moffett Field, California, USA.

tation Experiment (HALOE) instrument [e.g., Müller *et al.*, 1997]. During SOLVE, measurements of O<sub>3</sub> and various tracers were obtained by the Observations of the Middle Stratosphere (OMS) balloon-borne in situ and remote instrument payloads (the focus of this paper) and by instruments on the NASA ER-2 aircraft [Richard *et al.*, 2001]. The second method for quantifying chemical loss of ozone, the “vortex-averaged descent” technique, is based on analysis of the temporal evolution of O<sub>3</sub> on surfaces of potential temperature that descend according to rates calculated by a radiative model [e.g., Hoppel *et al.*, 2002]. The third method, the “Match” technique, relies on calculations of air parcel trajectories, which include diabatic descent, to follow the temporal evolution of O<sub>3</sub> for the same air parcels sampled at various times and places by a large number of coordinated ozonesonde soundings [e.g., Rex *et al.*, 1997].

[4] The present study focuses first on quantification of chemical loss of column O<sub>3</sub> using the “ozone versus tracer” technique applied to OMS measurements obtained between late November 1999 and 5 March 2000. These observations are then used to address concerns that have been expressed in the literature [e.g., Hall and Prather, 1995; Michelsen *et al.*, 1998; Plumb *et al.*, 2000] regarding the validity of this method for estimating chemical ozone loss. Finally, we compare chemical loss found using this approach with estimates from the “vortex-averaged descent” technique [Hoppel *et al.*, 2002] and the “Match” method [Rex *et al.*, 2002] to assess the overall validity of our quantitative understanding of chemical loss of column ozone.

## 2. Measurement and Instrument Descriptions

[5] The three balloon flights used here originated from a launch facility at Esrange, Sweden (67.9°N, 21.1°E). The two OMS in situ flights occurred on 991119 (Nov. 19, 1999; YYMMDD format is used throughout) and 000305. The in situ platform carries instruments such as a gas chromatograph and a UV-absorption photometer that determine atmospheric composition by directly sampling ambient air. The OMS remote flight used in our analysis took place on 991203. This platform carries instruments such as a Fourier Transform Infrared (FTIR) Spectrometer that determines atmospheric composition by recording high-resolution absorption spectra at various altitudes (tangent heights) as the sun rises or sets. All three flights sampled the core of the Arctic vortex, as shown in Figure 1. Throughout, we use “core” to refer to the inner 50% area of the vortex based on isolines of PV. For the November and December 1999 balloon flights, the PV analysis is conducted on the 550 K potential temperature ( $\theta$ ) surface. For the March 2000 balloon observations, the PV analysis is conducted on the  $\theta = 480$  K surface, reflecting in a gross manner the overall descent of the vortex during winter. The assessment of the location of each balloon flight relative to the structure of the vortex is insensitive to the particular isentropic level of the PV maps.

[6] A second OMS remote flight occurred on 000315, just prior to vortex break up. The sampled air masses are within the core of the vortex based on PV analyses (Figure 1). The temperature of the air masses sampled on 000315, between altitudes of 20 to 30 km, is about 10 to 20 K higher than conditions encountered on 000305. Examination of tracer profiles observed on 000315 shows that, for potential

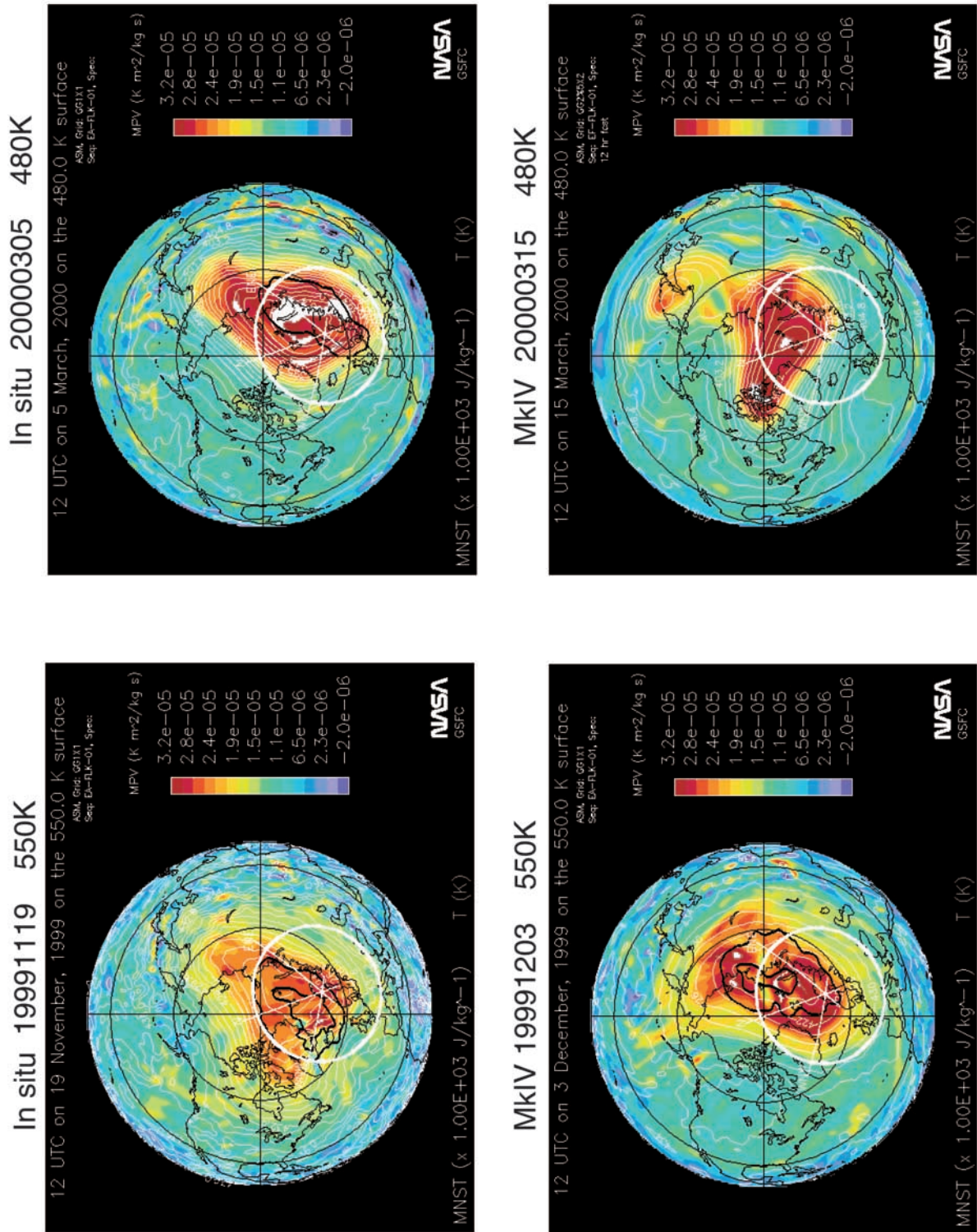
temperatures less than about 460 K, the sampled air might not have been in the core of the vortex (see section 4.3.2). Although the measurements made on the second OMS remote flight are of high quality, they are not used here since our focus is on ozone loss in the vortex core.

[7] The JPL balloon-borne ozone instrument is virtually identical to the ozone instrument on the NASA ER-2 aircraft [Proffitt and McLaughlin, 1983]. Ozone is measured in two chambers, one containing unperturbed air, the other containing air scrubbed of ozone. The ratio of the absorption of 254 nm radiation (generated by a single mercury lamp) in the two chambers is measured simultaneously, canceling out lamp intensity fluctuations. This ratio, coupled with the well-known O<sub>3</sub> absorption cross section and the temperature (controlled and easily measured), pressure, and path length of the chambers is used to determine the mixing ratio of O<sub>3</sub> in ambient air. The pressure of the chambers and of ambient air is measured with MKS Baratron (10, 100, 1000 torr ranges) regularly calibrated on a NIST-traceable calibration system and intercompared during flight. The mixing ratio of O<sub>3</sub> is reported every second with an overall uncertainty (accuracy and precision) of 3 to 5%. The ER-2 dual-beam UV-absorption ozone photometer obtains measurements of the abundance of O<sub>3</sub> at comparable levels of accuracy and precision [Proffitt *et al.*, 1989].

[8] The Lightweight Airborne Chromatography Experiment (LACE) that flew on the OMS in situ payload obtained measurements of a number of long-lived tracers, including N<sub>2</sub>O and CH<sub>4</sub>, with a precision of 1 to 3% and an accuracy of 1 to 4% [Ray *et al.*, 1999; Moore *et al.*, 2002]. The LACE measurements of [N<sub>2</sub>O] are used to define the chemical loss of O<sub>3</sub> because these observations were obtained at twice the vertical resolution of [CH<sub>4</sub>] ( $[X]$  is used to denote the volume mixing ratio of species  $x$  throughout). Similar estimates for chemical loss of O<sub>3</sub> are found, however, using LACE observations of [CH<sub>4</sub>] to define initial and final relations. Observations obtained during both ascent and descent are used throughout. They exhibit no significant difference, although data obtained during ascent span a considerably larger range of altitudes (i.e., provide coverage of the upper troposphere and lowermost stratosphere) than the descent data, due to the speed of the balloon during descent. The measurements of [N<sub>2</sub>O] from the NASA ER-2 aircraft used here were obtained by the Airborne Chromatograph for Atmospheric Trace Species (ACATS) instrument with precisions and accuracies that are comparable to the measurements from LACE [Elkins *et al.*, 1996; Romashkin *et al.*, 2001]. Measurements of atmospheric species by ACATS and LACE are reported as dry mole fractions based on calibrated gravimetric standard mixtures [Elkins *et al.*, 1996; Moore *et al.*, 2002].

[9] The OMS remote observations were obtained by the MkIV solar occultation FTIR spectrometer [Toon *et al.*, 1999] during sunset, when the instrument was at a float altitude of  $\sim 34$  km. The estimated  $1\sigma$  precision and accuracy of the O<sub>3</sub>, N<sub>2</sub>O, CH<sub>4</sub>, and CFC-11 observations are 1.7% and 6%, 1.0% and 3%, 1.4% and 5%, and 6.0% and 10%, respectively (error bars for MkIV measurements shown in the figures represent total uncertainty, found by combining the estimated precision and accuracy in a root sum of squares fashion). MkIV measurements of these species have been shown to compare well to observations

# PV Maps for SOLVE/OMS Esrance Balloon Flights



from the NASA ER-2 aircraft and other instruments [Sen *et al.*, 1998, 1999; Toon *et al.*, 1999].

[10] The temperature profile for the OMS in situ flight of 991119 was measured by a thermistor that is part of the ozone instrument. For 000305, we use the temperature profile measured by a radiosonde that was attached to the OMS gondola. The temperature profile for the OMS remote flight on 991203 is based on analysis of temperature sensitive CO<sub>2</sub> features in the recorded spectra [Sen *et al.*, 1998], augmented for altitudes below 400 mbar by sonde measurements from Esrange made immediately prior to the OMS launch. For all three OMS balloon flights, the measured temperature profiles compare quite well with profiles from the Goddard DAO (differences less than 3 K, for pressures between 10 and 200 mbar). Measurements of temperature and pressure from the ER-2 are obtained with total uncertainties of  $\pm 0.3$  K and  $\pm 0.25$  mbar, respectively, by the NASA Ames Meteorological Measurement System instrument [Scott *et al.*, 1990].

[11] Values for column O<sub>3</sub> throughout this study have been computed by evaluating the integral of [O<sub>3</sub>] versus pressure:

$$\text{ozone column (Dobson units)} = 0.794 \int_{p_1}^{973 \text{ mbar}} [\text{O}_3] dp, \quad (1)$$

where [O<sub>3</sub>] denotes the volume mixing ratio of ozone in parts per million and  $p$  denotes pressure in millibars (mbar). We have used this formalism to compute column O<sub>3</sub> because we have the greatest confidence in our directly measured values of O<sub>3</sub> mixing ratio and pressure (rather than altitude). For most estimates of total column O<sub>3</sub> reported here,  $p_1 = 8.9$  mbar, the uppermost altitude of the balloon flight on 000305. The integration limit of 973 mbar for equation (1) reflects the ground pressure at Esrange (surface elevation 271 m above sea level) on 000305 measured by the OMS ozone instrument. Equation (1) can be derived by substituting the hydrostatic balance relation [e.g., Holton, 1979, equation 1.14] into the standard equation for ozone column that is based on the integral of O<sub>3</sub> concentration versus altitude. The constant factor that appears outside of the integral is equal to:

$$\text{constant factor} = \frac{10^3 \times 10^{-6} \times R}{\text{DU}_{\text{conv}} \times k \times g}, \quad (2)$$

where the term  $10^3$  represents the conversion of pressure from units of dynes/cm<sup>2</sup> to mbar, the term  $10^{-6}$  accounts for the use of mixing ratio in parts per million,  $R$  is the gas constant for dry air,  $\text{DU}_{\text{conv}} = 2.687 \times 10^{16}$  molecules/cm<sup>2</sup> per Dobson unit,  $k$  is Boltzmann's constant, and  $g$  is the acceleration due to gravity (the variation of  $g$  with latitude and altitude is neglected because these variations have an insignificant effect on our calculations of chemical loss of ozone). Using CGS values for these parameters yields a value of 0.794 DU/(ppm  $\times$  mbar) for this factor.

### 3. Chemical Loss of Ozone

[12] The measured ozone profiles are shown in Figure 2a. The total column abundance of O<sub>3</sub> (denoted O<sub>3col</sub>) for

heights below 8.9 mbar on 000305 is 258 Dobson units (DU), which exceeds the O<sub>3col</sub> of 245 DU observed on 991119. The decrease in [O<sub>3</sub>] for  $100 < p < 30$  mbar observed on 000305, relative to 991119, is offset by an increase in [O<sub>3</sub>] at higher and lower altitudes. Air within the vortex has undergone considerable descent between 991119 and 000305, as indicated by the reduction in [N<sub>2</sub>O] at a given pressure level (Figure 2b). Considerable descent is also evident from profiles of [N<sub>2</sub>O] versus potential temperature (not shown). The local photochemical lifetime of N<sub>2</sub>O exceeds 300 yrs for  $p > 10$  mbar at 65°N during winter and consequently, in the absence of mixing, the initial [N<sub>2</sub>O] of an air parcel is preserved as air diabatically cools and descends. Since the mixing ratio of O<sub>3</sub> generally increases with increasing altitude, descent in the absence of chemistry would be expected to result in a significant increase in O<sub>3col</sub>, provided [O<sub>3</sub>] of air entering the top of the vortex exceeds [O<sub>3</sub>] of air leaving the bottom of the vortex. Indeed, for years with little or no PSC activity, the column abundance of Arctic O<sub>3</sub> typically increases by  $\sim 100$  DU throughout winter due to poleward, downward transport of ozone [e.g., Chipperfield, 1999].

[13] The evolution of the [O<sub>3</sub>] versus [N<sub>2</sub>O] relation (Figure 3) reveals that large amounts of chemical loss of O<sub>3</sub> occurred between 991119 and 000305. Isolated descent of purely vortex air, in the absence of chemical loss, should preserve the initial [O<sub>3</sub>] versus [N<sub>2</sub>O] relation [Plumb and Ko, 1992]. The observed [O<sub>3</sub>] versus [N<sub>2</sub>O] relations can be used to quantify the amount of chemical loss of O<sub>3</sub> in the column that occurred between the two balloon flights [e.g., Proffitt *et al.*, 1993; Müller *et al.*, 2001]. A profile for [O<sub>3</sub>] that is "reconstructed" by mapping the initial [O<sub>3</sub>] versus [N<sub>2</sub>O] relation onto the final [N<sub>2</sub>O] profile serves as a proxy, denoted [O<sub>3</sub>\*], for the abundance of O<sub>3</sub> that would have been present in the absence of any chemical loss. The chemical loss of O<sub>3</sub> throughout the column, denoted O<sub>3</sub> loss<sub>chem</sub>, is then found by computing the integral with respect to pressure of the difference between [O<sub>3</sub>\*] and measured [O<sub>3</sub>]:

$$\text{O}_3 \text{ loss}_{\text{chem}} \text{ (DU)} = 0.794 \int_{22.2 \text{ mbar}}^{118 \text{ mbar}} \left[ [\text{O}_3^*] - [\text{O}_3] \right] dp, \quad (3)$$

where [O<sub>3</sub>] is in parts per million and  $p$  is in mbar. A similar method for calculating chemical loss of column O<sub>3</sub> has been presented by Müller *et al.* [1997, 1999] using HALOE measurements of [O<sub>3</sub>] and [CH<sub>4</sub>].

[14] The integration limit of 118 mbar in equation (3) corresponds to an altitude of 14 km, which is at the 360 K potential temperature ( $\theta$ ) level on 000305. The 360 K level is used here to define the bottom of the Arctic vortex circulation system because, below this level, vortex and extravortex air parcels mix freely (as evidenced by similar values of [CFC-11] on isentropic surfaces, discussed in section 4.3.2). Below 360 K, it is unlikely that changes in [O<sub>3</sub>] are due to PSC related chemistry. Indeed, our analysis of simultaneous balloon-borne measurements of [CO<sub>2</sub>] at 1 Hz on 000305 (A. Andrews, private communication, 2001) reveals that most of the structure in [O<sub>3</sub>] below 118 mbar is dynamical in origin. The upper integration limit of 22.2 mbar corresponds to 24 km (about 590 K

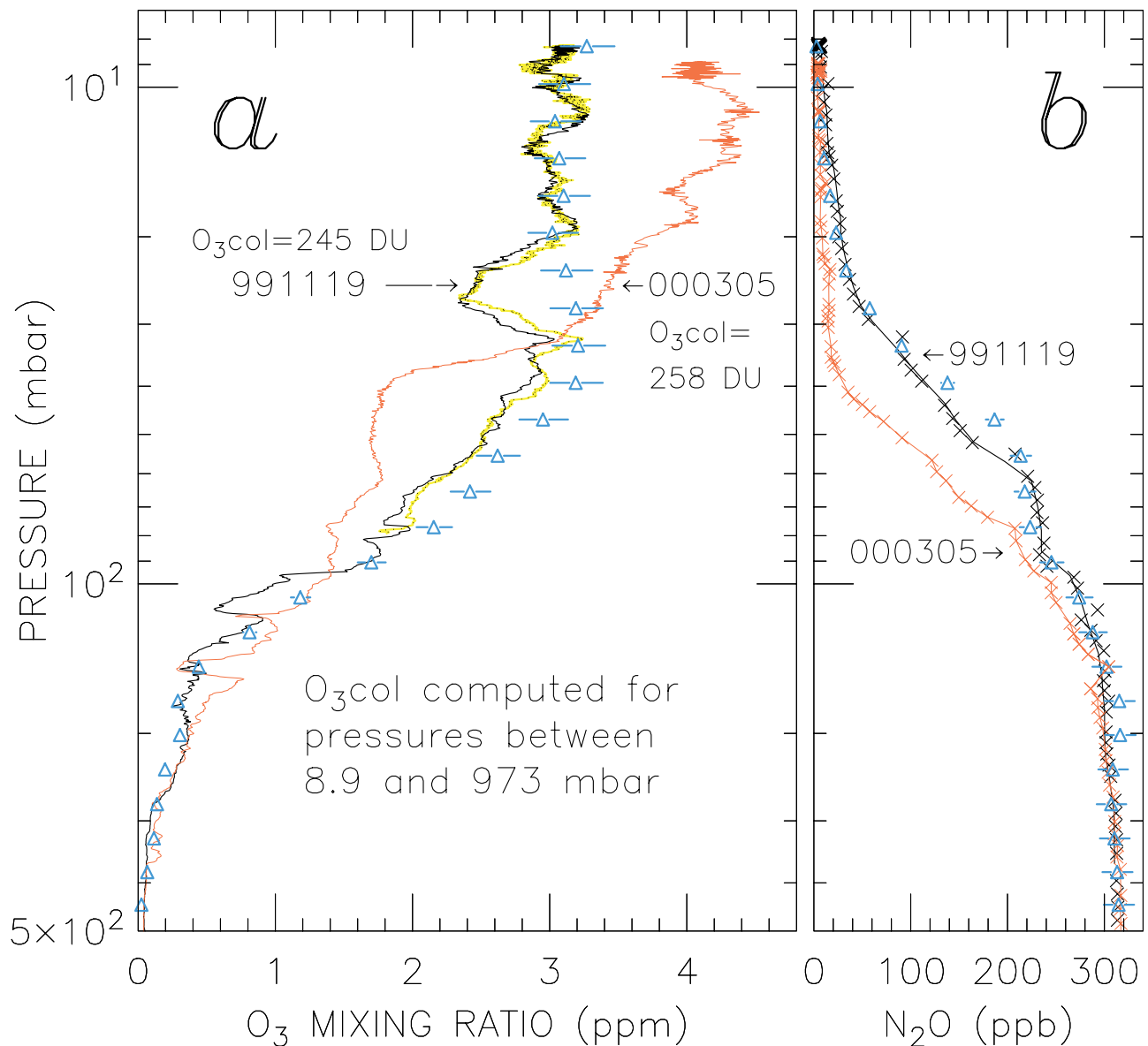


**Figure 2.** (a) Measurements of O<sub>3</sub> versus pressure in the Arctic vortex obtained by the OMS in situ ozone photometer on 991119 (black) and on 000305 (red) during ascent over Esrange, Sweden (67.9°N, 21.1°E). Profiles of O<sub>3</sub> measured during descent on 991119 (yellow dotted line) and by MkIV on 991203 (blue triangles) are also shown. (b) Measurements of N<sub>2</sub>O obtained by the LACE instrument on the two flights of the OMS in situ package (red and black crosses) and by MkIV on 991203 (blue triangles).

potential temperature), close to the highest altitude that PSCs and elevated ClO were observed during the Arctic winter of 1999/2000 [Bevilacqua *et al.*, 2002; Rex *et al.*, 2002]. This is also the highest altitude for which [O<sub>3</sub>\*] can be “reconstructed” from the measured mixing ratio of N<sub>2</sub>O on 000305.

[15] Evaluation of equation (3) leads to an estimate for O<sub>3</sub> loss<sub>chem</sub> of  $61 \pm 13$  DU for the time period between 991119 and 000305. The central value is based on a profile for [O<sub>3</sub>\*] found using the “mean” initial [O<sub>3</sub>] versus [N<sub>2</sub>O] relation shown in Figure 3. The largest source of uncertainty for O<sub>3</sub> loss<sub>chem</sub> is due to the initial [O<sub>3</sub>] versus [N<sub>2</sub>O] relation. A detailed discussion of the uncertainties in O<sub>3</sub> loss<sub>chem</sub>, including derivation of the  $\pm 13$  DU estimate, is given in section 4.

[16] Physically, the estimate of O<sub>3</sub> loss<sub>chem</sub> given by equation (3) represents the difference between the actual column abundance of O<sub>3</sub> that was observed on 000305 and the abundance of O<sub>3</sub> that would have been observed in the absence of any chemical loss provided air motions were unchanged. This quantity is most appropriately compared to the difference between “passive” ozone and “chemically active” ozone computed by three-dimensional model simulations [e.g., Deniel *et al.*, 1998]. It also serves as a measure of the effect of ozone depletion due to PSC-related halogen chemistry on the ultraviolet radiative environment below the Arctic vortex during 1999/2000.

[17] Chemical loss of ozone continued beyond 5 March 2000, the date of our last balloon measurement in the core of the vortex. Elevated levels of ClO existed in the vortex on 5

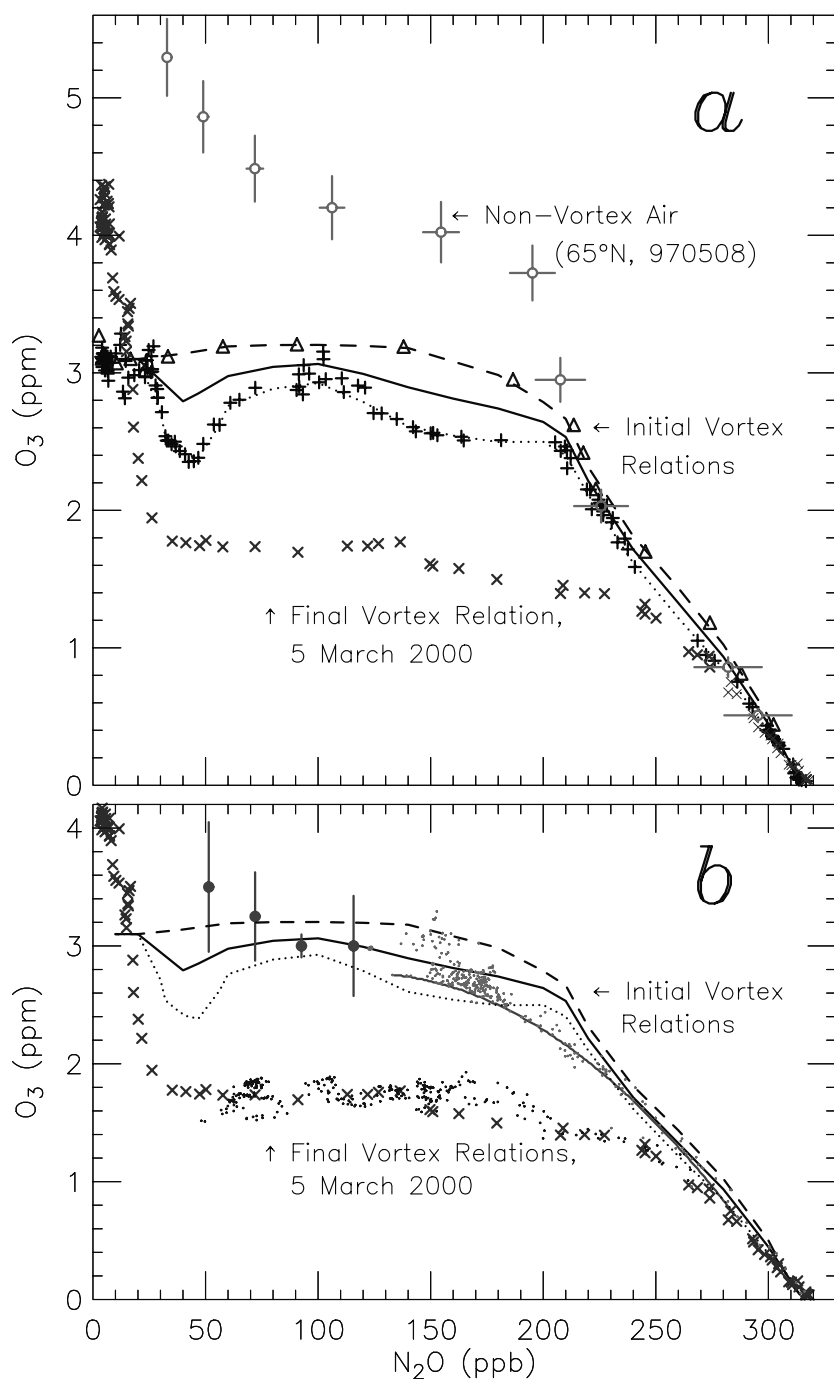


**Figure 3.** (a) Measurements of  $O_3$  versus  $N_2O$  in the Arctic vortex obtained by the balloon-borne ozone photometer and LACE on 991119 (black pluses) and 000305 (red crosses) and by the remote MkIV instrument on 991203 (blue triangles). Fits to three initial relations, used to estimate chemical loss of  $O_3$ , are shown by the black curves (in situ, dotted; remote, dashed; mean, solid). Observations obtained by MkIV on 970508 at high latitude, outside of the Arctic vortex, are also shown (green circles). Error bars denoting the total measurement uncertainty (accuracy plus precision) for the MkIV measurements of 970508 are shown. Error bars for the MkIV measurements on 991203 are comparable to those for 970508, and are not shown for clarity. (b) Fits to three initial relations for  $O_3$  versus  $N_2O$  (black lines) and the OMS in situ relation obtained on 000305 (red crosses) from Figure 3a, compared to ER-2 observations of  $O_3$  versus  $N_2O$  obtained in the Arctic vortex on 000120 (green dots) and on 000305 (blue dots). Also shown is the reference relation of Proffitt et al. [1993] based on ER-2 observations obtained during October 1991 (solid magenta line) and their "extrapolated" reference relation based on ozonesonde observations at higher altitudes (magenta points, with error bars representing the range of this relation). The value of  $N_2O$  associated with the Proffitt et al. relations has been increased by 2.9% to reflect its atmospheric increase between 1991 and 1999 [World Meteorological Organization, 1999].

March 2000 (R. Stimpfle, private communication, 2001). The Match analysis finds that  $O_3$  loss<sub>chem</sub> equaled  $88 \pm 13$  DU as of 26 March 2000 [Rex et al., 2002]. Sinnhuber et al. [2000], Hoppel et al. [2002], and Richard et al. [2001] also describe large amounts of chemical loss of Arctic  $O_3$  that extended beyond 5 March 2000, although none of these studies explicitly calculated chemical loss of column ozone. It is unlikely that significant PSC-related loss of column ozone took place after 26 March 2000. Minimum temperature in the vortex rose above the threshold for formation of PSCs on about 10 March 2000 [e.g., Manney and Sabutis, 2000; Rex et al., 2002] and our model calculations [e.g., Salawitch et al., 1993] indicate that the subsequent recovery of ClO to ClO<sub>2</sub> takes only two to three weeks, even for the highly denitrified conditions [e.g., Popp et al., 2001] observed this winter. Indeed, MLS observations show no evidence for high levels of [ClO] in the vortex on 27 to 29 March 2000 [Santee et al., 2000].

#### 4. Uncertainty of Chemical Loss of Ozone

[18] The estimate of  $O_3$  loss<sub>chem</sub> = 61 DU (between late November 1999 and 5 March 2000) given above is valid if the following conditions are met: 1) the initial  $[O_3]$  versus  $[N_2O]$  relation is representative of conditions throughout the core of the vortex; 2) the final  $[O_3]$  and  $[N_2O]$  profiles are representative of conditions throughout the core of the vortex; and 3) the  $[O_3]$  versus  $[N_2O]$  relation in the core of the vortex was not significantly influenced by dynamical processes during the course of winter. In the following sections, the effects of each condition on the uncertainty of  $O_3$  loss<sub>chem</sub> are quantified. It is shown that variability in the initial relation for  $[O_3]$  versus  $[N_2O]$  contributes  $\pm 11$  DU uncertainty to  $O_3$  loss<sub>chem</sub>, that variability in the final profile for  $[O_3]$  contributes an uncertainty of  $\pm 4$  DU, and that variability in the final profile for  $[N_2O]$  contributes  $\pm 4.7$  DU uncertainty. We also show, using a variety of tracer observations, that the  $[O_3]$  versus  $[N_2O]$  relation in the core of the vortex was not significantly influenced by transport. While we cannot show that the contributions to the uncertainty of  $O_3$  loss<sub>chem</sub> are independent, it is reasonable to calculate an overall uncertainty for  $O_3$  loss<sub>chem</sub> by combining the individual terms in a “root sum of squares” fashion. Consequently, we assign an overall uncertainty of  $\pm 13$  DU to  $O_3$  loss<sub>chem</sub>.

##### 4.1. Uncertainty Due to Initial Relations

[19] The initial  $[O_3]$  versus  $[N_2O]$  relation is used to estimate the final profile for  $[O_3^*]$ . Initial  $[O_3]$  versus  $[N_2O]$  relations measured by the in situ OMS package on 991119 (dotted line) and by the remote OMS package on 991203 (dashed line) are shown in Figure 3. The solid line, denoted the “mean” relation, is the average of the “in situ” and “remote” fits. Numerical values for the three initial relations are given in Table 1. The “mean” relation yields a value for  $O_3$  loss<sub>chem</sub> of 61 DU. The “in situ” and “remote” fits yield values of 50 and 72 DU, respectively. The rest of this section examines data from a variety of sources and concludes the differences between the “in situ” and “remote” initial relations are due primarily to atmospheric variability. Consequently, we assign an uncertainty of

**Table 1.** Initial Relation for  $[O_3]$  Versus  $[N_2O]^a$

$N_2O$ , ppb	$O_3$ In Situ, ppm	$O_3$ Remote, ppm	$O_3$ Mean, ppm
314	0.044	0.044	0.044
312	0.095	0.087	0.091
310	0.178	0.135	0.156
300	0.391	0.501	0.456
280	0.847	1.02	0.936
260	1.22	1.44	1.33
240	1.62	1.81	1.71
220	2.11	2.31	2.21
210	2.40	2.67	2.53
200	2.50	2.78	2.64
180	2.50	2.98	2.74
160	2.54	3.08	2.81
140	2.61	3.18	2.90
120	2.79	3.20	2.99
100	2.93	3.20	3.06
80	2.88	3.20	3.04
60	2.76	3.19	2.98
56.24	2.62	3.18	2.91
46.79	2.38	3.16	2.85
40.92	2.41	3.14	2.80
40	2.42	3.14	2.79
36.78	2.47	3.13	2.83
32.18	2.71	3.12	2.91
20	3.10	3.10	3.10

<sup>a</sup>The noninteger values of  $[N_2O]$  are required to capture the shape of the “notch” in  $[O_3]$  measured on 19 November 1999.

$\pm 11$  DU to  $O_3$  loss<sub>chem</sub> based on variability in the initial  $[O_3]$  versus  $[N_2O]$  relation.

[20] There are significant differences between the  $[O_3]$  versus  $[N_2O]$  relations measured on 991119 and 991203. Lower values of  $[O_3]$ , for the same value of  $[N_2O]$ , were observed on 991119 over an extended range of the relation (Figure 3). These differences can be traced primarily to the  $[O_3]$  profiles measured on the two flights (Figure 2). We focus first on differences for the range of the relations that can be compared directly to ER-2 observations in late January, i.e., the region for which  $[N_2O] > 120$  ppb.

[21] The first deep penetration of the Arctic vortex by the ER-2 aircraft during SOLVE occurred on 000120. The airplane sampled the core of the vortex at about the 440 K potential temperature level. Generally the  $[O_3]$  versus  $[N_2O]$  relation measured on 000120 lies within the range of the two balloon relations (Figure 3b). The ER-2 observations of  $[O_3]$  on 000120 are less than the OMS in situ initial relation for  $180 < [N_2O] < 230$  ppb (Figure 3b). This difference likely reflects chemical loss of  $O_3$  prior to 20 January 2000 [Rex et al., 2002]. Overall, the ER-2 observations in early January support the notion that the initial  $[O_3]$  versus  $[N_2O]$  relation was variable, and that the range of variability is well represented by the “remote” and “in situ” balloon data.

[22] A portion of the variability of the initial  $[O_3]$  versus  $[N_2O]$  measured by ER-2 instruments during late January 2000 can be ascribed to different relations being present on various potential temperature surfaces [Proffitt et al., 1993]. However, the primary differences between the balloon-borne observations on 991119 and 991203 are not due to this effect. Since we are limited to only three balloon-borne observations of  $[O_3]$  versus  $[N_2O]$ , any variations in initial conditions that might be accounted for by an isentropic analysis are folded into the uncertainty of  $O_3$  loss<sub>chem</sub>.

[23] We turn to a discussion of differences between the in situ and remote observations of  $[O_3]$  versus  $[N_2O]$  at higher altitudes (i.e., pressure <50 mbar). For  $[N_2O]$  between 100 and 170 ppb,  $[O_3]$  measured by the in situ photometer on 991119 is  $\sim 15\%$  less than  $[O_3]$  measured by MkIV on 991203 (Figure 3). Larger differences between the two measurements of  $[O_3]$  occur at  $[N_2O]$  of  $\sim 50$  ppb.

[24] Our analysis suggests these differences are also atmospheric in origin. The “notch” in  $[O_3]$  near 25 mbar on 991119 was present during both ascent and descent. The in situ and MkIV profiles of  $[O_3]$  converge for  $p < 20$  mbar and for  $p > 100$  mbar; that is, there is no evidence for instrumental artifacts at the highest or lowest altitudes of observation. Previous comparisons of MkIV and in situ measurements of  $[O_3]$  and  $[N_2O]$  reported differences less than 5% [Sen *et al.*, 1998; Toon *et al.*, 1999]. Furthermore, the in situ and MkIV profiles for  $[O_3]$  measured on 991119 and 991203, respectively, lie within the range of variability for  $[O_3]$  inside the vortex measured by the POAM III satellite instrument during late November 1999, as illustrated in Figures 4a and 4c. A detailed comparison of POAM III profiles of  $[O_3]$  obtained close to the time and place of the OMS measurements shows excellent agreement for all four OMS balloon flights, with differences typically less than 5% over a broad range of altitudes [Lumpe *et al.*, 2002].

[25] It is likely that the variability in  $[O_3]$  measured inside the vortex during late November and early December is due to local photochemistry not related to PSCs. Our model calculations constrained by long-lived radical precursors measured by MkIV on 991203 reveal that  $[O_3]$  is not in photochemical steady state at high latitudes during the time of vortex formation. For altitudes below 30 km, loss of  $O_3$  exceeds production because photolysis of  $O_2$  (at short wavelengths) essentially ceases but loss of  $O_3$  (driven by photolysis at longer wavelengths than  $O_2$  photolysis) proceeds, provided air is illuminated. The time constant to reach steady state is about five weeks at 30 km altitude (8 mbar),  $65^\circ N$  latitude, during early November. Consequently, the observed variability in profiles of  $[O_3]$  likely reflects differences in the recent photolytic history of the sampled air masses. This process would lead to differences in the  $[O_3]$  versus  $[N_2O]$  relation because profiles of  $[N_2O]$  are insensitive to recent photolytic history. A detailed examination of the profiles of  $[O_3]$  observed prior to the onset of PSC activity reaches similar conclusions [Kawa *et al.*, 2002].

#### 4.2. Uncertainty Due to Final Profiles

[26] The final profile for  $[O_3]$  measured on 000305 enters explicitly into the calculation of  $O_3$  loss<sub>chem</sub>. The final profile for  $[N_2O]$  enters this calculation implicitly via the dependence of  $[O_3^*]$  on  $[N_2O]$ . Our estimate of  $O_3$  loss<sub>chem</sub> is valid to the extent that the final profiles for  $[O_3]$  and  $[N_2O]$  are representative of conditions throughout the vortex.

[27] The representativeness of the final profile for  $[O_3]$  is assessed by comparison to data from ozonesondes, POAM III, and the ER-2. Our final profile for  $[O_3]$  tends to be a bit lower than a sonde profile for the “inner 25% area” of the vortex, as shown in section 5. Figures 4b and 4d show that the our final  $[O_3]$  profile lies toward the low end, but within the range of variability, of a profile from POAM III

averaged over the entire vortex. The ER-2 observations of  $[O_3]$  on 000305, obtained in a different part of the vortex, are nearly identical to our final  $[O_3]$  profile (Figure 5b). Use of the inner vortex sonde profile for  $[O_3]$  on 000305 results in a 4.0 DU reduction in our estimate of  $O_3$  loss<sub>chem</sub>. Consequently, we assign  $\pm 4$  DU uncertainty to  $O_3$  loss<sub>chem</sub> due to variability of the final profile of  $[O_3]$  in the vortex core.

[28] Portions of our final profile for  $[N_2O]$  are significantly lower ( $\sim 40$  ppb difference at 70 mbar) than a profile measured by the ACATS instrument on 000305 in the vortex core (Figure 6). Our final profile for  $[N_2O]$  agrees more closely with profiles of  $[N_2O]$  measured by ACATS during other ER-2 flights in the vortex core during the second ER-2 deployment of SOLVE (Figure 6), suggesting that the ACATS profile for  $[N_2O]$  on 000305 may have been influenced by air from outside the vortex or may represent a remnant of inhomogeneous descent within the vortex.

[29] The two profiles of  $[N_2O]$  are in better agreement if compared using potential temperature as a vertical coordinate, rather than pressure (Figure 6). Potential temperature is the more meaningful vertical coordinate upon which to base the comparisons of the balloon and aircraft profiles of  $[N_2O]$  because air parcels move isentropically as they traverse the vortex over short periods of time. In theory, the profile of  $[N_2O]$  versus pressure is the determining factor for our calculation of  $O_3$  loss<sub>chem</sub> due to the presence of pressure in equation (3). In practice, our calculation of  $O_3$  loss<sub>chem</sub> is rather insensitive to variations in  $[N_2O]$  on a pressure surface because the initial relation for  $[O_3]$  versus  $[N_2O]$  (used to estimate  $[O_3^*]$ ) is relatively flat.

[30] The observed variability of  $[N_2O]$  versus pressure in the core of the vortex during early March 2000 has a small effect on  $O_3$  loss<sub>chem</sub>. Use of the  $[N_2O]$  profile from the ER-2 flight segment on 000305 shown in Figure 6a, rather than the OMS profile for  $[N_2O]$  measured on 000305, results in a 4.7 DU reduction in the calculated column loss of  $O_3$ . The effect on  $O_3$  loss<sub>chem</sub> is small, despite at places substantial differences in  $[N_2O]$ , because these differences occur either for a region of the initial relation at which  $[O_3^*]$  is relatively insensitive to  $[N_2O]$  (i.e., for  $[N_2O] < 200$  ppb) or else for regions of the atmosphere (i.e.,  $90 < p < 120$  mbar) that do not contribute large amounts to  $O_3$  loss<sub>chem</sub>. We assign an uncertainty of  $\pm 4.7$  DU to  $O_3$  loss<sub>chem</sub> due to variability of the final  $[N_2O]$  profile in the core of the vortex.

#### 4.3. Effects of Transport on the $O_3$ Versus $N_2O$ Relation

[31] We now turn our attention to possible effects of dynamics on the  $[O_3]$  versus  $[N_2O]$  relation in the core of the vortex. Our estimate for  $O_3$  loss<sub>chem</sub> is valid only if the  $[O_3]$  versus  $[N_2O]$  relation in the core of the vortex was not significantly altered by dynamical processes between the initial and final days of measurement. Such dynamical processes include intrusions of nonvortex air across the wall of the vortex [Hall and Prather, 1995; Michelsen *et al.*, 1998; Plumb *et al.*, 2000] as well as rapid mixing of air parcels within the vortex [Ray *et al.*, 2002]. In the section below, we conclude that transport processes did not significantly alter the  $[O_3]$  versus  $[N_2O]$  relation in the core of the

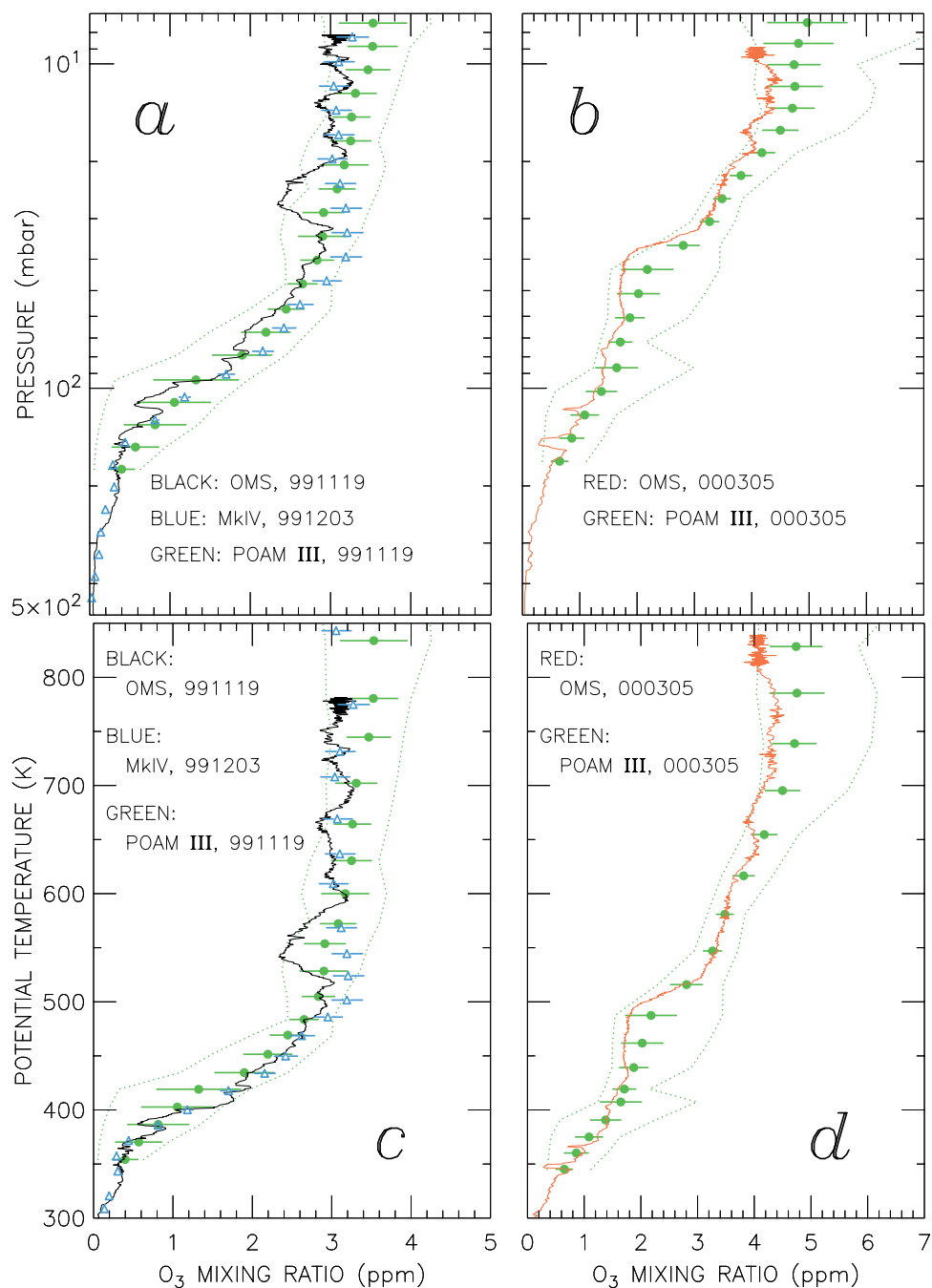


**Figure 4.** (a) Measurements of  $O_3$  versus pressure in the Arctic vortex obtained by the OMS in situ ozone photometer on 991119 (black) and by MkIV on 991203 (blue triangles) over Esrange, Sweden. Also shown are profiles of  $O_3$  from POAM III in the Arctic vortex for 991119  $\pm$  3 days (green). The circles and error bars represent the mean and standard deviation of the vortex average POAM III profile and the dotted lines show the maximum and minimum values measured over this time period. (b) Same as Figure 4a, except for the OMS in situ profile measured on 000305 and POAM III profiles of  $O_3$  averaged in the vortex within  $\pm$ 3 days of 000305. (c and d) Same as Figures 4a and 4b, respectively, except measurements are plotted versus potential temperature. Definition of whether the POAM III observations were in the vortex is based on the *Nash et al.* [1996] algorithm using PV analyses from the United Kingdom Meteorological Office (UKMO), as described by *Hoppel et al.* [2002]. The temperature and pressure profiles associated with the POAM III measurements are from UKMO analyses. All vortex averages of POAM III data were calculated on isentropic surfaces.

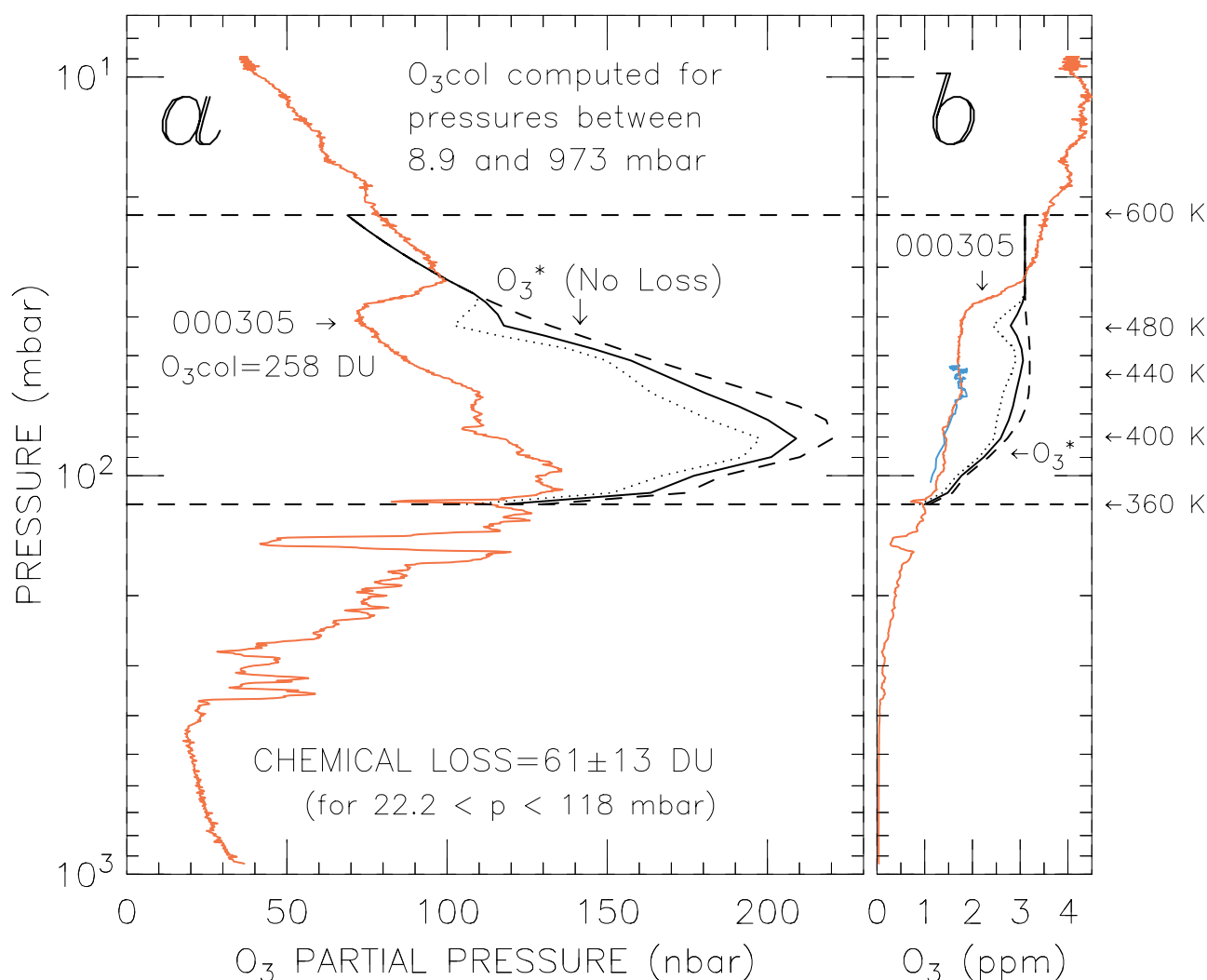


**Figure 5.** (a) Profile of O<sub>3</sub> measured by the OMS in situ photometer in the Arctic vortex on 000305 (red) compared to O<sub>3</sub><sup>\*</sup>, the profile of O<sub>3</sub> that would have been present in the absence of chemical loss (black lines). Three profiles for O<sub>3</sub><sup>\*</sup> are given, based on the profile of N<sub>2</sub>O measured by LACE on 000305 and the three fits to the initial O<sub>3</sub> versus N<sub>2</sub>O relation described in Figure 3. The partial pressure of O<sub>3</sub> is the product of the volume mixing ratio and atmospheric pressure. The area to the left of the profiles is proportional to the column abundance of O<sub>3</sub>. Chemical loss of O<sub>3</sub> has been found for pressures between 22.2 and 118 mbar (see section 3), as indicated by the dashed horizontal lines. (b) Same as Figure 5a, except profiles are shown as volume mixing ratio. The profile of O<sub>3</sub> measured by the ER-2 photometer in the core of the vortex on 000305 is also shown (blue). Potential temperatures corresponding to various pressure levels, for the balloon flight of 000305, are given in the right margin.

the Arctic vortex between 19 November 1999 and 5 March 2000.

#### 4.3.1. Intravortex Mixing

[32] “Intravortex mixing” refers here to irreversible mixing of various air parcels within the Arctic vortex that, due to inhomogeneous descent, could have once resided on the same isentropic level with quite different mixing ratios of N<sub>2</sub>O. This process can lead to the development of unique O<sub>3</sub> versus tracer relations within the Arctic vortex, potentially compromising the validity of our calculation of O<sub>3</sub> loss<sub>chem</sub> if the effects of intravortex mixing occur at the same time as chemical loss. We show below that intravortex mixing, which may have had a strong effect on the development of initial tracer relations in the vortex, did not affect our

estimate of O<sub>3</sub> loss<sub>chem</sub> because tracer fields were homogeneous during the time of rapid chemical loss.

[33] The OMS observations of [CH<sub>4</sub>] versus [N<sub>2</sub>O] provide important new information on the dynamics of the Arctic vortex. Similar, near-linear relations for [CH<sub>4</sub>] versus [N<sub>2</sub>O] (for values of [N<sub>2</sub>O] between ~50 and 250 ppb) were observed in the core of the vortex by LACE on 991119, by MkIV on 991203, and by LACE again on 000305 (Figure 7a). A curved relation between [CH<sub>4</sub>] and [N<sub>2</sub>O] is observed at high latitudes outside of the vortex [e.g., Herman *et al.*, 1998], illustrated in Figure 7a using MkIV observations from Fairbanks, Alaska (64.8°N, 147.6°W) obtained on 970508. It has generally been assumed that this curved relation would be found inside

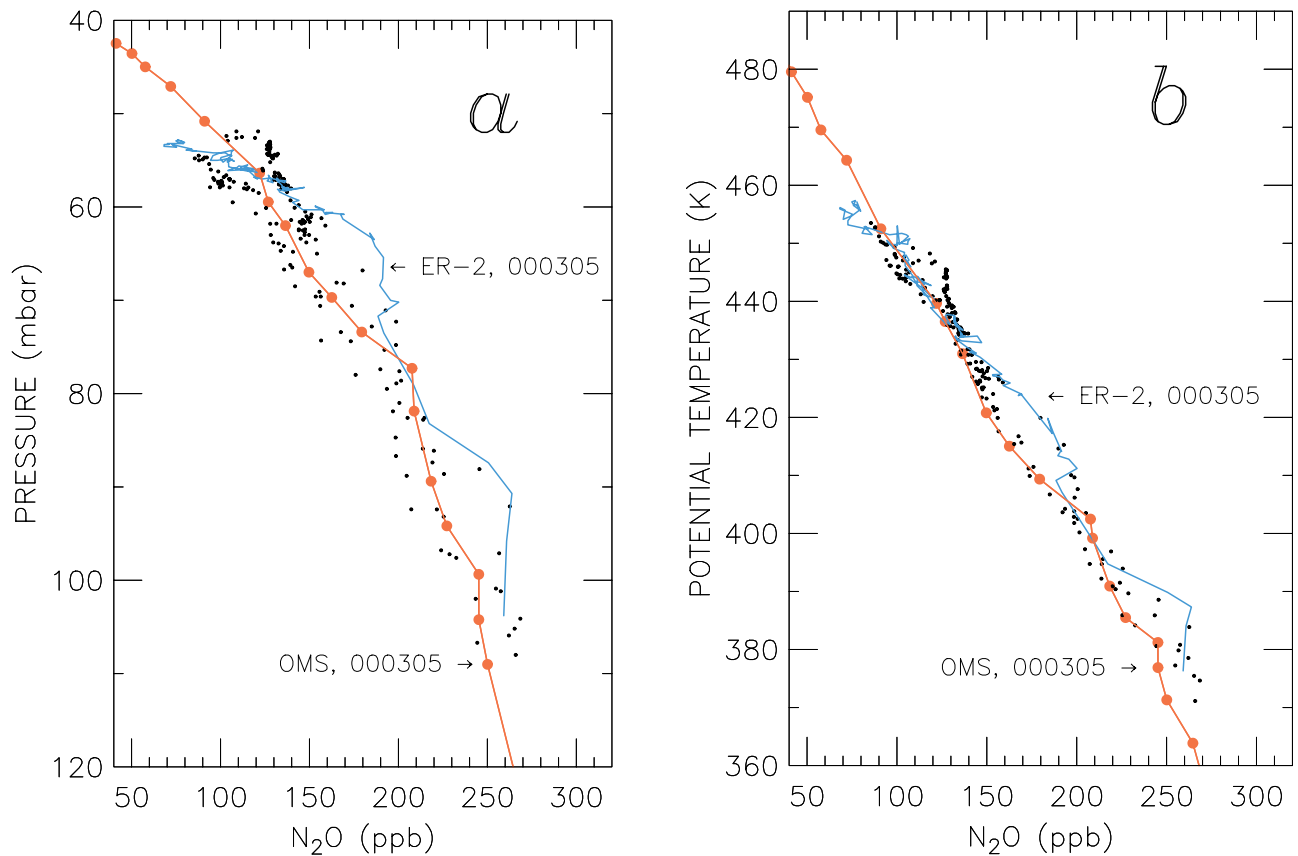


**Figure 6.** (a) The profile of  $\text{N}_2\text{O}$  versus pressure measured by the LACE balloon instrument in the Arctic vortex on 000305 (red) compared to profiles of  $\text{N}_2\text{O}$  measured by the ACATS ER-2 instrument on the same day (blue line) and for other flights of the ER-2 during its second deployment (black dots). All data are from the core of the vortex. The ACATS data shown in blue for 000305 were obtained during a slow climb starting at 11.18 Greenwich Mean Time (GMT) and ending at 14.10 GMT. All other ACATS observations, shown as black dots, were obtained during “dips” (descent, followed by ascent) of the ER-2 aircraft in the core of the vortex during the following times: 11.5 to 13.5 GMT on 000206; 10.15 to 11.18 GMT on 000305; 12.2 to 12.8 GMT on 000307; and 13.2 to 14.4 GMT on 000312. (b) Same as Figure 6a, except the profiles of  $\text{N}_2\text{O}$  are shown as a function of potential temperature.

the vortex during early winter [e.g., *Waugh et al.*, 1997; *Rex et al.*, 1999b]. Remarkably, the  $[\text{CH}_4]$  versus  $[\text{N}_2\text{O}]$  relation was observed to be linear soon after vortex formation. These observations may indicate that descent occurred in an inhomogeneous manner during the early formation period of the vortex and that subsequent, numerous irreversible mixing events within the isolated vortex led to a linearization of the relation as early as 991119 [*Ray et al.*, 2002]. Conversely, the observations might be due to rapid quasi-horizontal entrainment and permanent (irreversible) mixing of midlatitude air parcels with vortex air parcels during the incipient phase of vortex formation.

[34] The  $[\text{CH}_4]$  versus  $[\text{N}_2\text{O}]$  relation does not provide much guidance on intravortex mixing following the date of the initial observations. Once a tracer-tracer relation becomes linear, its shape cannot be changed by mixing unless air from a curved portion of the curve mixes with air from a linear portion of the curve. The subtle difference in the  $[\text{CH}_4]$  versus  $[\text{N}_2\text{O}]$  relation observed on 000305 at 480 K (Figure 7a) is probably due to intravortex mixing. If this is the case, such an event will have a negligible effect on our estimate of  $\text{O}_3$  loss<sub>chem</sub> because the ensemble of “end-

members” that would have led to this observation lie within the flat portion of the  $[\text{O}_3]$  versus  $[\text{N}_2\text{O}]$  relation.

[35] It is unlikely that intravortex mixing contributed to the evolution of the  $[\text{O}_3]$  versus  $[\text{N}_2\text{O}]$  relation subsequent to late January 2000 because tracer fields were homogeneous within the vortex during the time of rapid chemical loss. Profiles of  $[\text{N}_2\text{O}]$  measured in the vortex core indicate air parcels with  $\text{N}_2\text{O} \approx 100$  ppb were dynamically isolated from air parcels with  $\text{N}_2\text{O} \approx 250$  ppb during the time of rapid chemical loss of ozone. The mixing ratio of  $[\text{N}_2\text{O}]$  exhibits a relatively compact relation versus  $\theta$ . The dispersion of  $[\text{N}_2\text{O}]$  on an isentropic surface is no more than  $\sim 25$  ppb for five flights of the ER-2 in the vortex core between late February and mid March (Figure 6b). An analysis of data acquired during the first ER-2 deployment of SOLVE also shows small dispersion of  $[\text{N}_2\text{O}]$  on isentropic surfaces (not shown). Our analysis of  $[\text{N}_2\text{O}]$  measurements from two other instruments on the ER-2 (H. Jost, private communication, 2001; C. Webster, private communication, 2001) that provide observations of  $[\text{N}_2\text{O}]$  at higher time resolution than ACATS shows similarly small dispersion for  $[\text{N}_2\text{O}]$  on isentropic surfaces in the inner vortex. We lack sufficient measurements

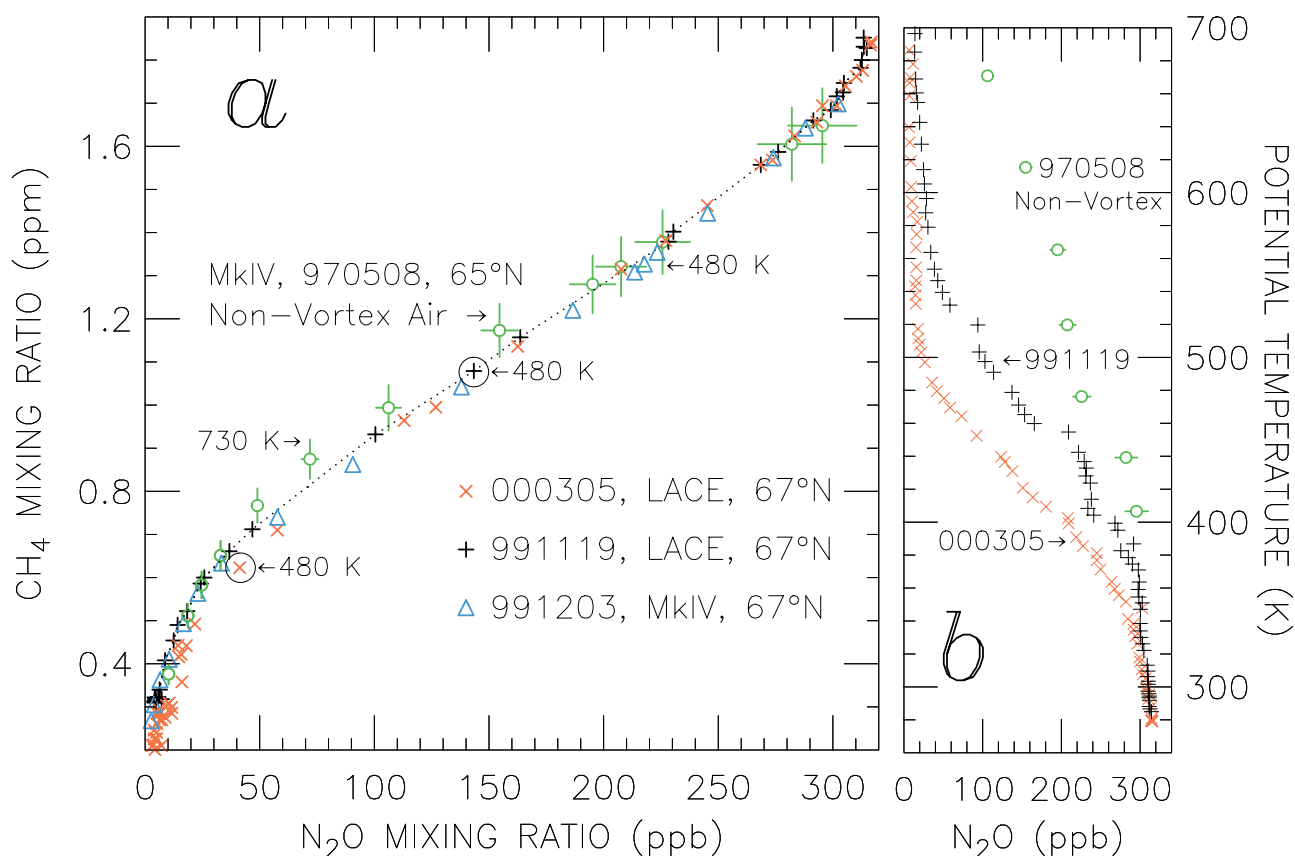


**Figure 7.** (a) Measurements of CH<sub>4</sub> versus N<sub>2</sub>O obtained in the Arctic vortex by the OMS in situ LACE instrument on 991119 (black pluses) and 000305 (red crosses) and by the OMS remote MkIV instrument in the vortex on 991203 (blue triangles) and outside the vortex on 970508 (green circles). Observations obtained on 970508, 991119, and 000305 at  $\theta = 480$  K, and on 970508 at 730 K, are marked. The dotted line connects the 991119 measurements for ease of interpretation. Error bars are only shown for the MkIV data obtained on 970508, as described in Figure 3. (b) Profiles of N<sub>2</sub>O versus potential temperature.

of [N<sub>2</sub>O] to make an empirical assessment of its dispersion above ER-2 altitudes. However, the relatively smooth decline of [N<sub>2</sub>O] with increasing  $\theta$  (Figure 7b) and the flat shape of the initial [O<sub>3</sub>] versus [N<sub>2</sub>O] relation strongly suggest intravortex mixing did not appreciably alter the relation at higher altitudes, for [N<sub>2</sub>O] greater than  $\sim 30$  ppb.

[36] Further insight into possible effects of intravortex mixing can be gained by examining the [O<sub>3</sub>] versus [N<sub>2</sub>O] relation (Figure 3). The OMS observations show that for the winter of 1999/2000, the initial relation was essentially “flat” (i.e., nearly constant [O<sub>3</sub>]) for  $50 < [\text{N}_2\text{O}] < 200$  ppb. There is an offset between the in situ and MkIV values of [O<sub>3</sub>] for the flat region of the initial relation that, if representative of true variability within the core of the vortex, would likely be smoothed out by intravortex mixing. The effect of this process on O<sub>3</sub> loss<sub>chem</sub> is represented by the  $\pm 11$  DU uncertainty due to variability in initial relations. Irreversible mixing between air parcels from the flat and the sloped regions of the initial relation may have led to a “rounding off” of the relation by late January 2000 [Ray *et al.*, 2002]. Use in equation (3) of the ER-2 relation for [O<sub>3</sub>] versus [N<sub>2</sub>O] measured on 000120, which appears to have been “rounded off”, leads to a 2 DU lower estimate for O<sub>3</sub> loss<sub>chem</sub>. This effect is insignificant given the larger overall uncertainties in O<sub>3</sub> loss<sub>chem</sub>.

[37] It is possible that our analysis results in a slight underestimation of O<sub>3</sub> loss<sub>chem</sub> due to intravortex mixing of air parcels that have descended by different amounts, for regions of the relation between [N<sub>2</sub>O] of 20 to 30 ppb. It is difficult to quantify empirically the magnitude of this effect, but it is small (i.e., less than 2 to 3 DU) because the transition of [O<sub>3</sub>] versus [N<sub>2</sub>O] from “flat” to “sloped” occurs over such a narrow region of [N<sub>2</sub>O] space. Again, we have neglected this possible underestimation of O<sub>3</sub> loss<sub>chem</sub> because it is so small.

#### 4.3.2. Entrainment

[38] “Entrainment” refers here to the irreversible mixing of air parcels from outside the vortex with air parcels inside the vortex, following the isentropic entrainment of the extravortex parcels into the vortex. Plumb *et al.* [2000] showed that slow, near-continuous entrainment of small amounts of nonvortex air can lead to the development of unique tracer-tracer relations within the vortex, due only to transport processes.

[39] An analysis of ER-2 measurements of [O<sub>3</sub>] and observations of [N<sub>2</sub>O] obtained at high temporal resolution shows evidence for infrequent entrainment of extravortex air at relatively small spatial scales, for limited regions of the outer vortex [Rex *et al.*, 2002, Figure 10]. These observations indicate that after the initial [O<sub>3</sub>] versus

[N<sub>2</sub>O] relation had been established, any quasi-horizontal mixing of air parcels across the edge of the vortex would have led to an increase in [O<sub>3</sub>] for the region of the relation that is used to quantify chemical loss. The ER-2 observations show for the Arctic winter of 1999/2000 that entrainment, if important, would lead to an underestimation of the true value of O<sub>3</sub> loss<sub>chem</sub> by our method.

[40] Observations of [CFC-11] and [N<sub>2</sub>O] obtained by the OMS instruments (Figure 8) provide compelling evidence that the vortex was essentially isolated from intrusions of extravortex air. Measurements of [CFC-11] and [N<sub>2</sub>O] observed by MkIV on 970508 for air at high-latitudes, outside of the remaining remnant of the polar vortex on that day, are also shown in Figure 8. The observations in the vortex core show near zero levels (mixing ratios less than 5 ppt) of [CFC-11] for  $\theta > 460$  K (Figure 8b). Observations from MkIV, LACE, and ACATS reveal much higher levels of [CFC-11] for nonvortex air at similar  $\theta$  levels. If nonvortex air had been entrained into the vortex, it would not be possible to maintain near zero [CFC-11] at 460 K and above.

[41] For air parcels below 460 K on 000305, there is a small difference in the [CFC-11] versus [N<sub>2</sub>O] relation relative to measurements obtained on 991119. We have quantitatively evaluated the degree of possible entrainment based on a simple mixing line analysis of the relations between [CFC-11], [N<sub>2</sub>O], and  $\theta$  measured by LACE on 991119 (initial vortex), by LACE on 000305 (final vortex), and by MkIV on 970508 and ACATS on 000316 (nonvortex air). We conclude that if the entrainment had occurred during the time of rapid chemical loss, nonvortex air parcels may have contributed at most 4 to 8% total contribution to the final composition of vortex air. This degree of entrainment would result in a small (e.g., several DU) underestimation of O<sub>3</sub> loss<sub>chem</sub>. Richard *et al.* [2001] reach a similar conclusion regarding isolation of the vortex from entrainment of nonvortex air based on an analysis of relations between [O<sub>3</sub>], [N<sub>2</sub>O], and [CO<sub>2</sub>]. Although multiple mixing events [Plumb *et al.*, 2000] would have led to slightly larger fractional contributions of nonvortex air to the final composition of the vortex based on the above [CFC-11] versus [N<sub>2</sub>O] analysis, it is difficult to conceive of appreciable changes occurring to the [O<sub>3</sub>] versus [N<sub>2</sub>O] relation due to entrainment without substantial changes also being recorded in the [CFC-11] versus [N<sub>2</sub>O] relation. Simply put, the contrast between vortex and nonvortex [CFC-11] on isentropic surfaces is much larger than the contrast between vortex and nonvortex [O<sub>3</sub>].

[42] Several other aspects of vortex dynamics can be gleaned from the data shown in Figure 8b. The ensemble of [CFC-11] versus  $\theta$  observations support the identification of 360 K as the bottom of the vortex circulation system for our calculation of O<sub>3</sub> loss<sub>chem</sub>. The high data point for [CFC-11] at 350 K (about 150 mbar) on 000305 is associated with “dynamical shear” and supports the contention that the structure in [O<sub>3</sub>] found at 150 mbar on 000305 (Figure 5a) was due to transport. A plot of [CFC-11] versus  $\theta$  for ER-2 observations obtained on 000226, 000305, 000307, and 000312 (light blue dots) looks remarkably similar to the OMS measurements made on 000305. Thus, the OMS in situ observations of the [CFC-11] profile on 000305 are a robust feature of the core of the vortex during

late winter 1999/2000. Finally, the OMS remote observations of [CFC-11] versus  $\theta$  obtained on 000315 (dark blue  $\nabla$ , Figure 8b) suggest that, for potential temperature levels below 460 K, these air parcels may not be representative of conditions in the vortex core (data from this flight are not used in our analysis of O<sub>3</sub> loss<sub>chem</sub>).

[43] We turn our attention to model results presented by Plumb *et al.* [2000, Plates 2 and 3]. They showed that, within a model, it was possible to generate shapes of a “stratospheric source gas” (their  $\chi_2$  tracer) versus “tropospheric source gas” ( $\chi_1$  tracer) that change during winter in a manner somewhat similar to our observations of [O<sub>3</sub>] and [N<sub>2</sub>O], due only to transport-related processes. Plumb *et al.* state that their heuristic model calculations are appropriate for understanding stratospheric measurements of [NO<sub>y</sub>] and [N<sub>2</sub>O] in the vortex; they do not directly apply the results of this calculation to the interpretation of stratospheric observations of [O<sub>3</sub>] versus [N<sub>2</sub>O]. However, Plumb *et al.* [2000, p. 100,409] do state “estimates of ozone depletion inferred from O<sub>3</sub>:tracer relations are likely to be overestimates” due to effects of mixing. We believe some confusion may presently exist in the community due to the use, by others, of these model calculations for interpretation of measurements of [O<sub>3</sub>] and [N<sub>2</sub>O].

[44] The Plumb *et al.* [2000] model results for  $\chi_2$  versus  $\chi_1$  are driven primarily by supply of air at the top of the vortex with near zero mixing ratios of both species. Our observations exhibit a critical difference with respect to these heuristic model calculations. The OMS measurements show that the top of the Arctic vortex is supplied with air having mixing ratios of O<sub>3</sub> between 3 and 4 ppm, considerably higher than the final value of [O<sub>3</sub>] in the inner vortex. The POAM III observations of [O<sub>3</sub>] shown in Figures 4a and 4c, which represent a significantly larger number of air masses, lead to the same conclusion. It is not possible to “feed” the top of the Arctic vortex with air having near zero mixing ratios of [O<sub>3</sub>]. Even though air depleted in both O<sub>3</sub> and N<sub>2</sub>O exists in the mesosphere, our photochemical model calculations [e.g., Osterman *et al.*, 1997], for constraints from the MkIV flight on 991203, indicate that O<sub>3</sub> is quickly regenerated to mixing ratios of 3 to 4 ppm by normal gas phase photochemistry as these air parcels pass through the 40 km level (the photochemical time constant for O<sub>3</sub> is less than 1 week, even at high latitudes during winter). Our observations show that supply of O<sub>3</sub> depleted air into the top of the vortex did not play a role in the subsequent evolution of the [O<sub>3</sub>] versus [N<sub>2</sub>O] relation. Therefore the model results of Plumb *et al.* for  $\chi_2$  versus  $\chi_1$  should not be applied to the interpretation of [O<sub>3</sub>] versus [N<sub>2</sub>O] within the Arctic vortex. As mentioned above, ER-2 observations for the Arctic winter of 1999/2000 show that the small amount of entrainment that did occur leads to a slight underestimation of the true value of O<sub>3</sub> loss<sub>chem</sub> by our method.

## 5. Comparison With Other Estimates of Chemical Loss

[45] An important goal articulated during the early planning stages of SOLVE/THESEO 2000 was to compare a variety of approaches that estimate chemical ozone loss to assess the validity of each method. In sections 5.1 and 5.2, we compare O<sub>3</sub> loss<sub>chem</sub> found using the balloon obser-

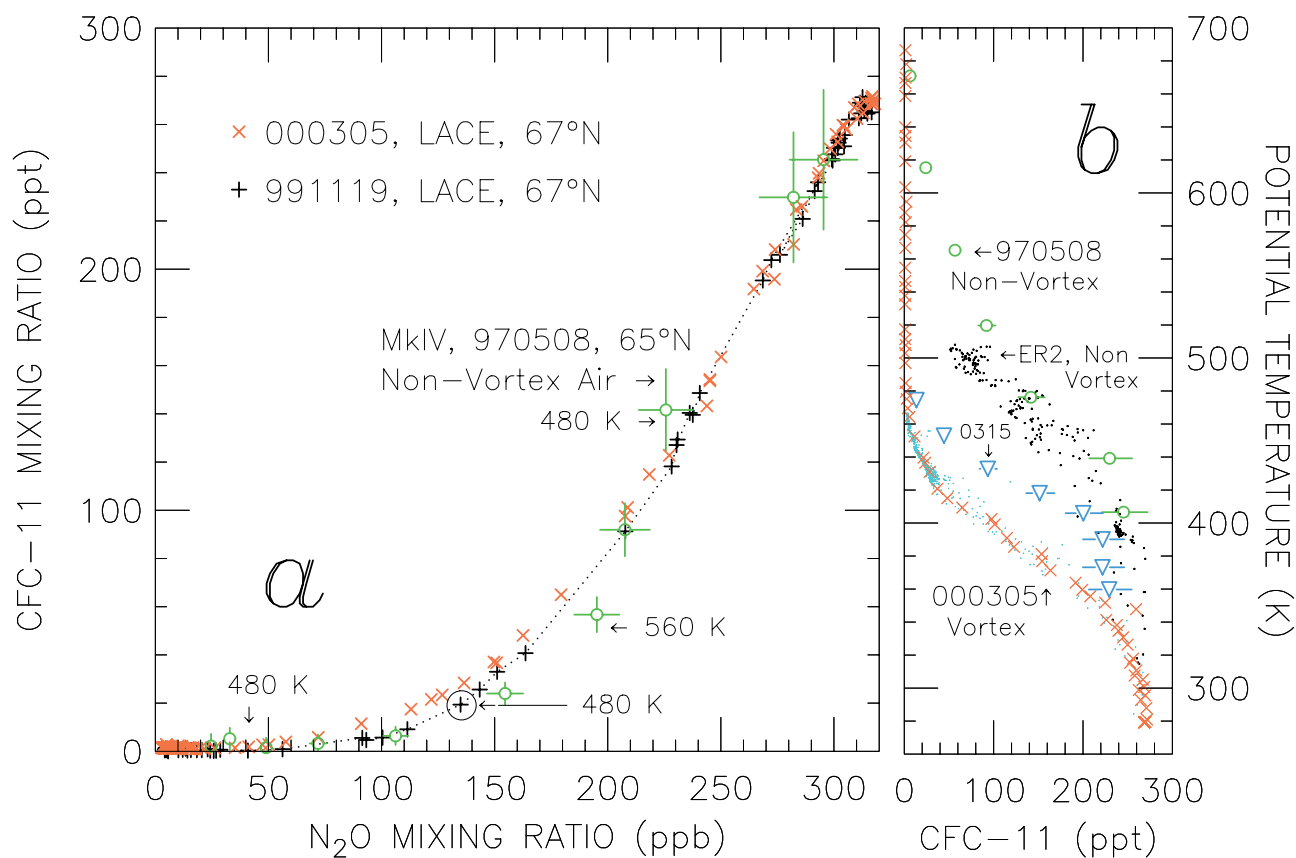


**Figure 8.** (a) Measurements of CFC-11 versus N<sub>2</sub>O obtained in the Arctic vortex by the OMS in situ LACE instrument on 991119 (black plusses) and 000305 (red crosses) and by the OMS remote MkIV instrument outside the vortex on 970508 (green circles). Observations obtained on 970508, 991119, and 000305 at  $\theta = 480$  K, and on 970508 at 560 K, are marked. The dotted line connects the 991119 measurements for ease of interpretation. Error bars are only shown for the MkIV data obtained on 970508, as described in Figure 3. (b) Profiles of CFC-11 versus potential temperature, measured by MkIV on 970508 (green circles) and by LACE on 000305 (red crosses). Also shown are measurements obtained by the ACATS instrument aboard the ER-2 aircraft on 991211 and 000316 (black dots), two flights that sampled air entirely outside of the polar vortex based on analyses of potential vorticity, and on 000226, 000307, 000305, and 000312 (light blue points), four flights that sampled the vortex core (time segments are the same as given in Figure 6). Finally, observations obtained by MkIV on 000315 from Esrange, Sweden are also shown (dark blue triangles).

Measurements of CFC-11 versus N<sub>2</sub>O obtained in the Arctic vortex by the OMS in situ LACE instrument on 991119 (black plusses) and 000305 (red crosses) and by the OMS remote MkIV instrument outside the vortex on 970508 (green circles). Observations obtained on 970508, 991119, and 000305 at  $\theta = 480$  K, and on 970508 at 560 K, are marked. The dotted line connects the 991119 measurements for ease of interpretation. Error bars are only shown for the MkIV data obtained on 970508, as described in Figure 3. (b) Profiles of CFC-11 versus potential temperature, measured by MkIV on 970508 (green circles) and by LACE on 000305 (red crosses). Also shown are measurements obtained by the ACATS instrument aboard the ER-2 aircraft on 991211 and 000316 (black dots), two flights that sampled air entirely outside of the polar vortex based on analyses of potential vorticity, and on 000226, 000307, 000305, and 000312 (light blue points), four flights that sampled the vortex core (time segments are the same as given in Figure 6). Finally, observations obtained by MkIV on 000315 from Esrange, Sweden are also shown (dark blue triangles).

Measurements of CFC-11 versus N<sub>2</sub>O obtained in the Arctic vortex by the OMS in situ LACE instrument on 991119 (black plusses) and 000305 (red crosses) and by the OMS remote MkIV instrument outside the vortex on 970508 (green circles). Observations obtained on 970508, 991119, and 000305 at  $\theta = 480$  K, and on 970508 at 560 K, are marked. The dotted line connects the 991119 measurements for ease of interpretation. Error bars are only shown for the MkIV data obtained on 970508, as described in Figure 3. (b) Profiles of CFC-11 versus potential temperature, measured by MkIV on 970508 (green circles) and by LACE on 000305 (red crosses). Also shown are measurements obtained by the ACATS instrument aboard the ER-2 aircraft on 991211 and 000316 (black dots), two flights that sampled air entirely outside of the polar vortex based on analyses of potential vorticity, and on 000226, 000307, 000305, and 000312 (light blue points), four flights that sampled the vortex core (time segments are the same as given in Figure 6). Finally, observations obtained by MkIV on 000315 from Esrange, Sweden are also shown (dark blue triangles).

Measurements of CFC-11 versus N<sub>2</sub>O obtained in the Arctic vortex by the OMS in situ LACE instrument on 991119 (black plusses) and 000305 (red crosses) and by the OMS remote MkIV instrument outside the vortex on 970508 (green circles). Observations obtained on 970508, 991119, and 000305 at  $\theta = 480$  K, and on 970508 at 560 K, are marked. The dotted line connects the 991119 measurements for ease of interpretation. Error bars are only shown for the MkIV data obtained on 970508, as described in Figure 3. (b) Profiles of CFC-11 versus potential temperature, measured by MkIV on 970508 (green circles) and by LACE on 000305 (red crosses). Also shown are measurements obtained by the ACATS instrument aboard the ER-2 aircraft on 991211 and 000316 (black dots), two flights that sampled air entirely outside of the polar vortex based on analyses of potential vorticity, and on 000226, 000307, 000305, and 000312 (light blue points), four flights that sampled the vortex core (time segments are the same as given in Figure 6). Finally, observations obtained by MkIV on 000315 from Esrange, Sweden are also shown (dark blue triangles).

### 5.1. Comparison With POAM III

[46] Calculations of O<sub>3</sub> loss<sub>chem</sub> from the Polar Ozone and Aerosol Measurement (POAM) III satellite instrument of the U.S. Naval Research Laboratory [Lucke *et al.*, 1999], which is similar to the NASA SAGE II instrument [McCormick *et al.*, 1989], provide an important opportunity to

accomplish a key goal of SOLVE. The estimates of O<sub>3</sub> loss<sub>chem</sub> from POAM III used here are obtained by the “vortex-averaged descent” technique [Hoppel *et al.*, 2002]. Chemical loss is determined based on the temporal evolution of O<sub>3</sub> measured on surfaces of potential temperature that descend according to rates calculated by a radiative model [Hoppel *et al.*, 2002]. It is assumed that the dynamical contribution to changes in O<sub>3</sub> column within the vortex are dominated by diabatic descent. Changes in [O<sub>3</sub>] due to entrainment of extravortex air are not accounted for. Also, it is assumed that descent within the vortex can be adequately represented in a “vortex-averaged sense”.

[47] Vortex-averaged profiles of [O<sub>3</sub>] and [O<sub>3</sub>\*] for 000305 from POAM III are compared with OMS balloon-based profiles in Figure 9a (here we use [O<sub>3</sub>] to refer to O<sub>3</sub> mixing ratio and to O<sub>3</sub> partial pressure interchangeably). The POAM III profile for [O<sub>3</sub>\*] is found by allowing a vortex-averaged profile for [O<sub>3</sub>] measured in early January to descend diabatically until 5 March, using heating rates

for this winter from the SLIMCAT model [Chipperfield, 1999]. Further discussion of these profiles is given in section 5.2.

[48] An important test of our quantitative understanding of Arctic ozone is provided by comparing calculations of  $O_3$  loss<sub>chem</sub> found using the OMS balloon-based “ozone versus tracer” method with estimates found using the POAM III-based “vortex-averaged descent” method. Chemical loss from the OMS balloon-borne is  $61 \pm 13$  DU as of 000305, as described in section 3. Applying equation (3) to the POAM III profiles of  $[O_3]$  and  $[O_3^*]$  results in a value for  $O_3$  loss<sub>chem</sub> of  $51 \pm 11$  DU, for the vortex as a whole as of 000305. The uncertainty estimate for the POAM III calculation of  $O_3$  loss<sub>chem</sub> is based on the  $1\sigma$  standard deviation of the vortex-averaged profile of  $[O_3]$  on 000305. Care must be taken in comparing estimates of chemical  $O_3$  loss<sub>chem</sub> for the core of the vortex (balloon observations) to estimates for the vortex as a whole (POAM III observations) because the actual chemical loss rates could vary due to different degrees of sun-light exposure and temperature histories that would affect details of chlorine activation, chlorine recovery, and daily ozone loss rates [e.g., Harris *et al.*, 2002]. Given this caveat, the two estimates of chemical loss are in good agreement (differences within the respective uncertainties). A key goal of SOLVE, the validation of a solar occultation satellite instrument measurement of ozone loss, has therefore been accomplished, albeit with a different satellite instrument than originally planned.

## 5.2. Comparison With Ozonesondes

[49] A Match campaign consisting of measurements of  $[O_3]$  from a total of 770 ozonesondes, launched from 29 stations, was carried out during the THESEO 2000 [Rex *et al.*, 2002]. The ozonesonde launches were coordinated in real time to probe several hundreds of air masses twice over a several-day interval (so-called “Match events”). Chemical loss rates are calculated from a statistical analysis of changes in ozone from many Match events. Synoptic scale intrusions of extravortex air are explicitly accounted for by the Match method, and great care is taken to avoid areas of potential small scale mixing. Further details are provided by Rex *et al.* [1997, 1999a, 2002, and references therein].

[50] The chemical loss of column  $O_3$  found by Match as of 000305 was  $53 \pm 12$  DU [Rex *et al.*, 2002]. The uncertainty represents the  $1\sigma$  standard deviation to the statistical fit of the variations in  $O_3$  for various Match events. The Match estimate for chemical loss of column  $O_3$  is in good agreement (differences within the respective uncertainties) with both the OMS balloon-based and the POAM III satellite-based estimates for  $O_3$  loss<sub>chem</sub> (Table 2).

[51] The red curves in Figure 9b show  $[O_3]$  and  $[O_3^*]$  from OMS for 000305, as discussed above. The solid green curve represents the vortex-averaged profile of  $[O_3]$  on 000305 from the ozonesondes (calculations of  $O_3$  loss<sub>chem</sub> found by applying the “vortex-averaged descent” method to these sonde profiles are in excellent agreement with estimates based on the “Match” method [Rex *et al.*, 2002]). The dashed green curve is a profile for  $[O_3^*]$  on 000305, found by allowing the vortex-averaged profile for early January to descend diabatically until 5 March using heating rates from SLIMCAT [Rex *et al.*, 2002]. Finally, the dotted green line

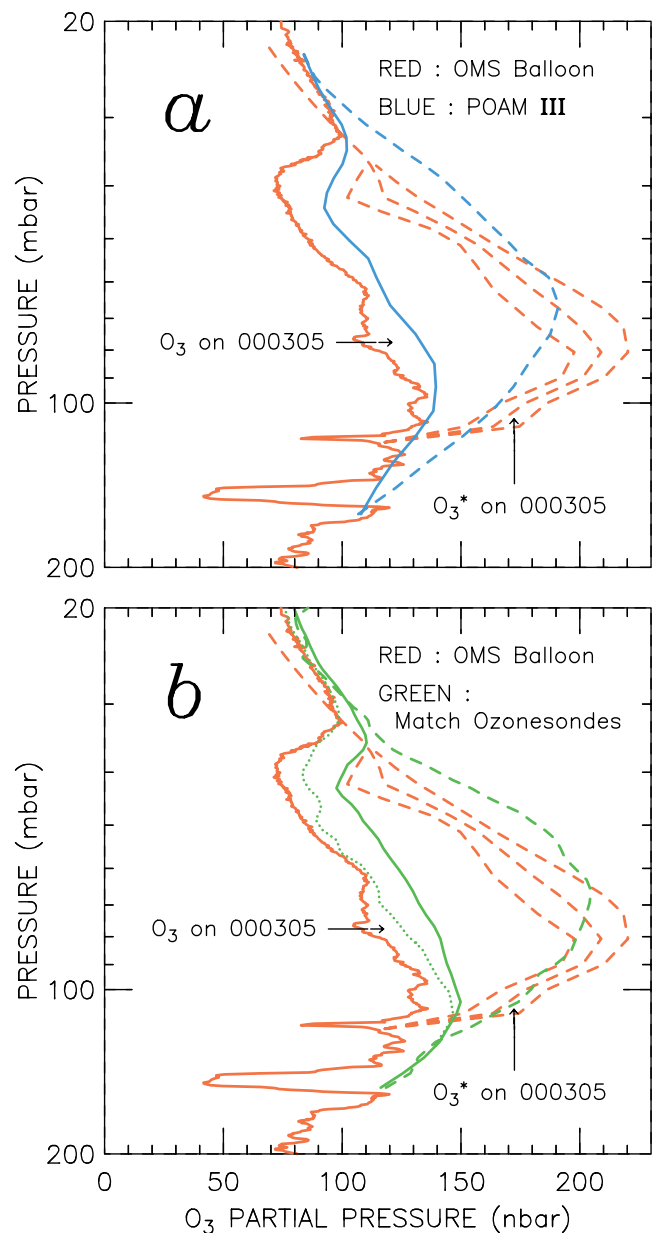


**Figure 9.** (a) The profile of  $O_3$  measured by the OMS in situ photometer in the Arctic vortex on 000305 (red solid) and the three estimates of  $O_3^*$  from Figure 5 (red dashed). Also shown are POAM III profiles for 000305 of vortex-averaged  $O_3$  (blue solid) and of  $O_3^*$  (blue dashed), calculated by allowing a vortex-averaged profile of  $O_3$  measured in early January to descend (see section 5.1). (b) Same as Figure 9a, except profiles of  $O_3$  (vortex-averaged; green solid) and  $O_3^*$  (green dashed) are based on measurements inside the Arctic vortex from Match ozonesondes. Also shown is a profile of  $O_3$  from the Match sondes for the innermost 25% area of the vortex on 000305 (green dotted).

represents an averaged profile for 000305 from the sondes for the inner 25% area of the vortex.

[52] The agreement between the POAM III (Figure 9a) and ozonesonde (Figure 9b) profiles of both  $[O_3]$  and  $[O_3^*]$  is remarkable. Both represent “vortex-averaged” conditions. Hoppel *et al.* [2002] and Rex *et al.* [2002] each show

that the comparisons between POAM III and ozonesonde estimates of  $O_3$  loss\_chem,  $[O_3]$ , and  $[O_3^*]$  remain in excellent agreement up to 15 March 2000, the last date the vortex could be sampled by POAM III. Since profiles for  $[O_3]$  and  $[O_3^*]$  for 000305 from POAM III and the ozonesondes are so similar, these profiles are referred as the “POAM/sonde” profiles in the next paragraph.

[53] Differences between the POAM/sonde profiles and the OMS profiles for  $[O_3]$  and  $[O_3^*]$  are relatively small. Estimates of  $O_3$  loss\_chem from OMS, POAM III, and the ozonesondes are in reasonable agreement despite these differences. Most of the difference between the OMS profiles and the POAM/sonde profiles of  $[O_3]$  is due to structure within the vortex on 000305. A profile of  $[O_3]$  for 000305 from the ozonesondes, computed by only averaging data collected in the inner 25% of the vortex, is in much closer agreement with the OMS profile (green dotted line, Figure 9b). Therefore it is likely that differences between the POAM/sonde value for  $O_3$  loss\_chem and the value found using OMS data reflects atmospheric variability in chemical loss between the core of the vortex versus loss averaged throughout the vortex.

### 5.3. Comparison With HALOE

[54] The HALOE instrument measures profiles of  $O_3$ ,  $H_2O$ ,  $NO_2$ ,  $HCl$ ,  $HF$ , and  $CH_4$  using solar occultation [Russell *et al.*, 1993]. The latitudinal coverage of HALOE varies, reaching as high as about  $55^\circ N$  during late January 1996 and as high as  $60^\circ N$  during early March 1995 [e.g., Müller *et al.*, 1999, Figure 1]. Müller *et al.* [1997, 1999, and references therein] have estimated  $O_3$  loss\_chem from HALOE measurements of  $O_3$  and  $CH_4$  using a procedure that is similar to that applied here to the OMS balloon observations. For the winter of 1995/1996, they reported that chemical processes in the Arctic vortex reduced column ozone by 120 to 160 DU [Müller *et al.*, 1997]. Estimates of  $O_3$  loss\_chem from HALOE are unavailable for winter of 1999/2000 due to a lack of initial relation measurements in the vortex.

[55] Comparison of the HALOE reference relations for  $[O_3]$  versus  $[CH_4]$  to initial conditions measured in the core of the Arctic vortex by the OMS instruments is warranted because of concerns that the early winter HALOE measurements may not be truly representative of vortex composition [e.g., Michelsen *et al.*, 1998]. Due to limitations imposed by the UARS orbit, these early winter reference relations are obtained at relatively low latitudes. For the ozone loss calculations applied to the winter of 1995/1996, the early winter reference relation was based on measurements made at  $47^\circ N$  during November 1995 and at  $49^\circ N$  during January 1996 [Müller *et al.*, 1997, 1999]. Maps of potential vorticity indicate these early winter HALOE observations were obtained inside the Arctic vortex, and profiles of  $[CH_4]$  versus potential temperature for these occultations show clear evidence of local descent [Müller *et al.*, 1999].

[56] Figure 10 shows the relation between  $[O_3]$  versus  $[CH_4]$  measured in the vortex core by LACE on 991119 (+) and by MkIV ( $\Delta$ ) on 991203. Also shown is a measurement of  $[O_3]$  versus  $[CH_4]$  for nonvortex air sampled by MkIV over Fairbanks, Alaska ( $64.8^\circ N$ ,  $147.6^\circ W$ ) on 970508 ( $\circ$ ). Finally, early winter HALOE reference relations for  $[O_3]$  versus  $[CH_4]$  from five winters, starting with 1991/1992 and

**Table 2.** Comparisons of Chemical Loss of Column Ozone,  $O_3$  loss\_chem, Inside the Arctic Vortex for the Winter of 1999/2000 as of 5 March 2000

Data Source	OMS Balloon	POAM III Satellite	Ozonesondes
Method	tracer-tracer ( $O_3$ versus $N_2O$ )	vortex-averaged descent	Match trajectory analysis
$O_3$ loss_chem	$61 \pm 13$ DU	$51 \pm 11$ DU	$53 \pm 12$ DU

ending with 1995/1996, are also shown (dashed lines) in Figure 10. These relations were computed using the formula given in Table 3 of Müller *et al.* [1999] and reflect fits to version 18 HALOE data. Although atmospheric  $CH_4$  has increased between 1991 and 1999, we do not account for this increase in Figure 10 because it has no effect on the comparisons.

[57] The HALOE early winter reference relations for  $[O_3]$  versus  $[CH_4]$  are substantially higher than the OMS relations measured during the winter of 1999/2000. For levels of  $[CH_4]$  equal to about 0.5 ppm, the OMS instruments (both the in situ photometer and the MkIV FTIR) report  $O_3$  mixing ratios of about 3.0 ppm. The HALOE reference relation peaks at  $O_3 \approx 4.5$  ppm for this level of  $[CH_4]$ . It is possible that this difference reflects true year-to-year variability in the set up conditions of the Arctic vortex. It is also possible, however, that the discrepancy indicates the HALOE observations were either near the edge of the vortex or otherwise strongly influenced by extravortex air parcels, particularly at higher altitudes (i.e.,  $\theta > 480$  K, where  $[CH_4]$  from OMS is  $< 1.0$  ppm). The early winter HALOE reference relations are similar to the relation between  $[O_3]$  versus  $[CH_4]$  measured by MkIV for non-vortex air over Fairbanks, Alaska (Figure 10). Observations from HALOE obtained during late winter and early spring (used to define final  $[O_3]$ ) are clearly located in the inner vortex, as evidenced by the very low amounts of  $[HCl]$  associated with these occultations. However, the comparison of the OMS initial  $[O_3]$  versus  $[CH_4]$  observed during SOLVE to the HALOE initial relations casts doubt on the reliability of the HALOE-based estimates of chemical loss of column ozone. Further investigations are necessary of the validity of the early winter HALOE reference relations, their usefulness for quantitative assessments of  $O_3$  loss\_chem, and possible year to year variability in Arctic vortex set up conditions.

### 5.4. Comparison With ER-2 Observations

[58] Richard *et al.* [2001] have presented an analysis of chemical loss of  $O_3$  in the lower stratosphere for the Arctic winter of 1999/2000, based on the temporal evolution of the  $[O_3]$  versus  $[N_2O]$  relation from ER-2 observations. The Richard *et al.* loss estimates are given in terms of mixing ratio (termed here “local loss”). The ER-2 observations do not extend to high enough altitudes to allow for estimates of column loss. We ascribe larger uncertainty to the initial relation for  $[O_3]$  versus  $[N_2O]$  than is given by Richard *et al.*, based on the variability in  $[O_3]$  measured in the vortex core by the two early balloon flights and by POAM III (section 4.1). There is remarkably good agreement between the ER-2 and balloon measurements of  $[O_3]$  versus  $[N_2O]$  on 000305 (Figure 3b). The similarity of the relation derived from vertical sampling by the balloon platform and primarily horizontal sampling by the aircraft addresses

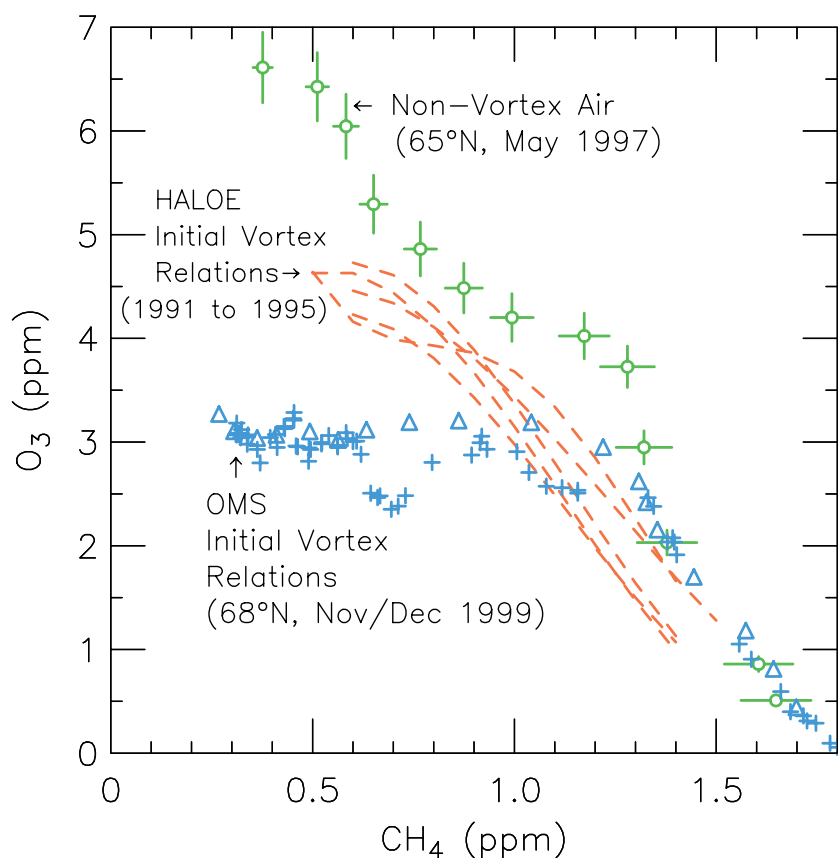


**Figure 10.** Measurements of  $O_3$  versus  $CH_4$  in the core of the Arctic vortex obtained by LACE on 991119 (blue plusses) by MkIV on 991203 (blue triangles). Observations obtained by MkIV on 970508 at high latitude, outside of the Arctic vortex, are also shown (green circles). Error bars denoting the total measurement uncertainty (accuracy plus precision) for the MkIV measurements of 970508 are shown. Error bars for the MkIV measurements on 991203 are comparable to those for 970508, and are not shown for clarity. Error bars for total measurement uncertainty of the LACE observations are small, about 3 to 5%, and are not shown. Also shown are early vortex reference relations for  $O_3$  versus  $CH_4$  based on version 18 observations from HALOE for five winters starting in 1991/1992 and ending in 1995/1996, computed using formulas given by Müller *et al.* [1999, Table 3] (red dashed lines).

a concern raised by Hall and Prather [1995] and demonstrates the suitability of the combined use of both data sources for studies of polar ozone loss. The ER-2 last sampled the vortex on 000312. Examining these data in terms of our initial relations for  $[O_3]$  versus  $[N_2O]$ , we infer a local chemical loss of  $1.76 \pm 0.21$  ppmv for air at 450 K on 000312. This value compares well with estimates of local chemical loss at 450 K found by many other methods [Newman *et al.*, 2002].

[59] Our final comparison is to early winter reference relations for  $[O_3]$  versus  $[N_2O]$  used by Proffitt *et al.* [1993] to quantify chemical loss of Arctic ozone. Concern has been raised regarding the validity of the Proffitt *et al.* early winter reference relations because, for values of  $[N_2O]$  less than  $\sim 130$  ppb, the relations are not based on simultaneous observation of both tracers in the vortex [e.g., Müller *et al.*, 2001, and references therein].

[60] The portion of the Proffitt *et al.* [1993] reference relation based on ER-2 observations in the vortex is shown by the solid magenta line in Figure 3b. Proffitt *et al.* extended their early winter reference relation to  $[N_2O] = 50$  ppb based on ozonesonde observations and an extrapolation

of ER-2 observations of  $[N_2O]$  versus  $\theta$  (points with error bars in Figure 3b). The Proffitt *et al.* reference relation is in good overall agreement with our balloon based initial relation for the entire range of  $[N_2O]$ . For  $180 < [N_2O] < 230$  ppb, the Proffitt *et al.* reference relation (based on measurements in October) is somewhat lower than the OMS initial relation, but agrees well with ER-2 observations obtained on 000120. This raises the possibility that the actual variability of the initial relation in late November/early December is somewhat larger than we have allowed for. This difference has a 2 DU effect on  $O_3$  loss<sub>chem</sub>, so is negligible in terms of our overall estimates of chemical loss. Most importantly, our OMS balloon observations support the validity of the quantitative results for chemical loss of ozone given by Proffitt *et al.* [1993], subject to the caveat that 1991/1992 and 1999/2000 were dynamically different winters.

## 6. Concluding Remarks

[61] The Arctic winter of 1999/2000 was notable for the exceptional extent, in both space and time, of temperatures

cold enough to allow for the formation of PSCs [e.g., *Manney and Sabutis*, 2000; *Bevilacqua et al.*, 2002]. Elevated levels of [ClO] due to reactions on the surface of PSCs were observed over widespread areas of the vortex [e.g., *Rex et al.*, 2002].

[62] We have used balloon-borne observations of [O<sub>3</sub>] and [N<sub>2</sub>O] obtained by the JPL O<sub>3</sub> photometer, the NOAA LACE gas chromatograph, and the JPL MkIV FTIR to calculate that chemical loss of O<sub>3</sub> equaled 61 ± 13 DU, between 118 mbar and 22.2 mbar, in the core (i.e., inner 50%) of the vortex between 19 November 1999 and 5 March 2000. Our value for chemical loss of column ozone compares well (differences within uncertainty estimates) with other calculations of chemical loss for the vortex as a whole. As of 5 March, chemical loss found using the Match technique [*Rex et al.*, 2002], as applied to independent ozonesonde data, was 53 ± 12 DU. Loss found using the vortex-averaged descent technique [*Hoppel et al.*, 2002], as applied to profiles of [O<sub>3</sub>] measured by the POAM III satellite instrument, was 51 ± 11 DU. It is possible that the systematic difference between these estimates represents variability of chemical loss between the core of the vortex (tracer estimate) and the vortex as a whole (Match and POAM III estimates). Nonetheless, the overall comparison establishes the validity of each approach for estimating chemical loss of column ozone for the Arctic winter of 1999/2000.

[63] Chemical loss of ozone continued beyond 5 March 2000, the date of our last balloon measurement in the core of the vortex. Elevated levels of ClO existed in the vortex on 5 March 2000 (R. Stimpfle, private communication, 2002). The Match analysis finds that chemical loss of column ozone equaled 88 ± 13 DU as of 26 March 2000, the time of the last coordinated ozonesonde launches [*Rex et al.*, 2002].

[64] We have used the OMS balloon-borne observations to show that dynamical process could not have made a significant contribution to the observed change in the [O<sub>3</sub>] versus [N<sub>2</sub>O] relation during the winter of 1999/2000. The most important findings regarding the dynamics of the Arctic vortex based on our tracer observations are:

1. The vortex was essentially isolated from intrusions of midlatitude air, for the time and place of chemical loss of ozone, based on the observation of near zero mixing ratios of CFC-11 on 5 March 2000 (for θ above 460 K) and the small changes in the [CFC-11] versus [N<sub>2</sub>O] relation observed in the core of the vortex at all potential temperature levels between 11 November 1999 and 5 March 2000.

2. The early winter vortex reference relation for [O<sub>3</sub>] versus [N<sub>2</sub>O] was essentially “flat” (i.e., nearly constant [O<sub>3</sub>] for variable [N<sub>2</sub>O]) for the region of largest chemical loss (30 < [N<sub>2</sub>O] < 200 ppb). Air parcels with different values of [N<sub>2</sub>O] were dynamically isolated in the core of the vortex, based on the observation of quite low dispersion of [N<sub>2</sub>O] on isentropic surfaces. Therefore intravortex mixing during the time of rapid chemical loss of ozone was unlikely to have led to appreciable changes in the [O<sub>3</sub>] versus [N<sub>2</sub>O] relation.

3. The steep reductions in [O<sub>3</sub>] on surfaces of constant [N<sub>2</sub>O] observed during early March could not have been caused by transport. For transport to have led to these

changes, air with [O<sub>3</sub>] less than 1.8 ppm (the final mixing ratio) and near zero [N<sub>2</sub>O] must be mixed into the vortex. Although such air exists in the mesosphere, our observations indicate that [O<sub>3</sub>] was about 3 to 4 ppm for air supplied at the top of the vortex due to regeneration of O<sub>3</sub> as air descends through the 40 km altitude region. Simply put, there is no “end-member” at appropriate potential temperature levels that could possibly mix into the vortex and alter the [O<sub>3</sub>] versus [N<sub>2</sub>O] relation in a manner that would mimic massive chemical loss of ozone.

[65] The initial [O<sub>3</sub>] versus [CH<sub>4</sub>] measured inside the core of the Arctic vortex on 19 November 1999 and on 3 December 1999 is significantly lower ([O<sub>3</sub>] differences of ~1.5 ppm for values of [CH<sub>4</sub>] equal to about 0.5 ppm) than the suite of initial reference relations used by *Müller et al.* [1997, 1999, and references therein] to estimate chemical loss of column ozone for five winters based on HALOE data. *Müller et al.* [1999] show maps of PV that indicate these early winter HALOE observations were obtained inside the Arctic vortex; profiles of [CH<sub>4</sub>] versus θ for these occultations show evidence of local descent. Nonetheless, the HALOE observations used to define these initial reference relations are obtained at fairly low latitudes (e.g., 46 to 51°N for the winter of 1995/1996). One interpretation of the discrepancy is that the early winter HALOE observations were either on the edge of the vortex or were otherwise influenced by extravortex air parcels. Taken at face value, the OMS observations of [O<sub>3</sub>] versus [CH<sub>4</sub>] obtained during SOLVE suggest the HALOE-based estimates of chemical loss of column ozone may overestimate by significant amounts the true loss in the vortex core. This statement assumes that vortex set up conditions for the winter of 1999/2000 were relatively similar to conditions for previous years, an assumption that can not easily be tested by existing observations. Further investigation is required.

[66] The initial [O<sub>3</sub>] versus [N<sub>2</sub>O] relation measured inside the Arctic vortex during the winter of 1999/2000 agrees well with the initial reference relation used by *Proffitt et al.* [1993], even for the portion of their relation that was based on measurements of [O<sub>3</sub>] from sondes and “extrapolated [N<sub>2</sub>O]” from ER-2 observations. Our observations support the validity of the *Proffitt et al.* [1993] quantitative calculations of chemical loss of Arctic ozone, given the caveat that the dynamics governing the set up of the vortex may have been different for 1991/1992 than for 1999/2000.

[67] Finally, we end by noting our conclusion that the [O<sub>3</sub>] versus [N<sub>2</sub>O] relation was not affected by transport cannot necessarily be applied to other Arctic winters, particularly dynamically active years. If there is one lesson from the rich suite of measurements made over past years, it is that each Arctic winter is dynamically distinct.

[68] **Acknowledgments.** Research at the Jet Propulsion Laboratory, California Institute of Technology, is performed under contract with the National Aeronautics and Space Administration (NASA). This work was supported by the Upper Atmosphere Research Program, the Atmospheric Chemistry Modeling and Analysis Program, and the Atmospheric Effects of Aviation Program. The POAM III experiment is supported by the Office of Naval Research and the NASA Data Purchase Program. The ozonesondes used in THESEO 2000 were supported through the European Center Environment Programme. We appreciate the efforts and dedication of the National Scientific Balloon Facility personnel, the JPL Balloon Flight Support Group, the staff at the Esrange balloon launch facility, the ER-2 ground support crew, the ER-2 pilots, and the personnel at numerous

ozonesonde stations. We thank William Brune, OMS project scientist for SOLVE, and Paul Newman and James Anderson, ER-2 project scientists for SOLVE, for their excellent leadership throughout the mission. We thank Paul Newman and Leslie Lait for supplying the PV data shown here, and Leslie Lait and two anonymous reviewers for helpful comments on the manuscript.

## References

- Bevilacqua, R. M., et al., Observations and analysis of polar stratospheric clouds detected by POAM III during the 1999/2000 Northern Hemisphere winter, *J. Geophys. Res.*, *107*, doi:10.1029/2001JD000477, in press, 2002.
- Chipperfield, M. P., Multiannual simulations with a three-dimensional chemical transport model, *J. Geophys. Res.*, *104*, 1781–1805, 1999.
- Chipperfield, M. P., and R. L. Jones, Relative influence of atmospheric chemistry and transport on Arctic ozone trends, *Nature*, *400*, 551–554, 1999.
- Deniel, C., R. M. Bevilacqua, J. P. Pommereau, and F. Lefèvre, Arctic chemical ozone depletion during the 1994–1995 winter deduced from POAM II satellite observations and REPROBUS three-dimensional model, *J. Geophys. Res.*, *103*, 19,231–19,244, 1998.
- Elkins, J. W., et al., Airborne gas chromatograph for in situ measurements of long-lived species in the upper troposphere and lower stratosphere, *Geophys. Res. Lett.*, *23*, 347–350, 1996.
- Hall, T. M., and M. J. Prather, Seasonal evolutions of N<sub>2</sub>O, O<sub>3</sub>, and CO<sub>2</sub>: Three-dimensional simulations of stratospheric correlations, *J. Geophys. Res.*, *100*, 16,699–16,720, 1995.
- Harris, N. R. P., M. Rex, F. Goutail, B. M. Knudsen, G. L. Manney, R. Müller, and P. von der Gathen, Comparison of empirically derived ozone losses in the Arctic vortex, *J. Geophys. Res.*, *107*, doi:10.1029/2001JD000482, in press, 2002.
- Herman, R. L., et al., Tropical entrainment timescales inferred from stratospheric N<sub>2</sub>O and CH<sub>4</sub> observations, *Geophys. Res. Lett.*, *25*, 2781–2784, 1998.
- Holton, J. R., *An Introduction to Dynamic Meteorology*, 2nd ed., Academic, San Diego, Calif., 1979.
- Hoppel, K., R. M. Bevilacqua, G. Nedoluha, C. Deniel, F. Lefevre, J. D. Lumpe, M. D. Fromm, C. E. Randall, J. E. Rosenfield, and M. Rex, POAM III observations of arctic ozone loss for the 1999/2000 winter, *J. Geophys. Res.*, *107*, doi:10.1029/2001JD000476, in press, 2002.
- Kawa, S. R., R. M. Bevilacqua, J. J. Margitan, A. R. Douglass, M. R. Schoeberl, K. W. Hoppel, and B. Sen, Interaction between dynamics and chemistry of ozone in the setup phase of the Northern Hemisphere polar vortex, *J. Geophys. Res.*, *107*, doi:10.1029/2001JD001527, in press, 2002.
- Lucke, R. L., et al., The Polar Ozone and Aerosol Measurement (POAM) III instrument and early validation results, *J. Geophys. Res.*, *104*, 18,785–19,799, 1999.
- Lumpe, J. D., et al., Comparison of POAM III ozone measurements with correlative aircraft and balloon data during SOLVE, *J. Geophys. Res.*, *107*, doi:10.1029/2001JD000472, in press, 2002.
- Manney, G. L., and J. L. Sabutis, Development of the polar vortex in the 1999–2000 Arctic winter stratosphere, *Geophys. Res. Lett.*, *27*, 2589–2592, 2000.
- McCormick, M. P., J. M. Zawodny, R. E. Veiga, J. C. Larsen, and P. H. Wang, An overview of SAGE I and II ozone measurements, *Planet. Space Sci.*, *37*, 1567–1586, 1989.
- Michelsen, H. A., G. L. Manney, M. R. Gunson, and R. Zander, Correlations of stratospheric [NO<sub>y</sub>], [O<sub>3</sub>], [N<sub>2</sub>O], and [CH<sub>4</sub>] derived from ATMOS measurements, *J. Geophys. Res.*, *103*, 28,347–28,359, 1998.
- Moore, F. L., et al., Balloon-borne in situ gas chromatography for measurements in the troposphere and stratosphere, *J. Geophys. Res.*, *107*, doi:10.1029/2001JD000891, in press, 2002.
- Müller, R., P. J. Crutzen, J.-U. Groos, C. Brühl, J. M. Russell III, H. Germandt, D. S. McKenna, and A. F. Tuck, Record chemical ozone loss in the Arctic during the winter of 1995–96, *Nature*, *389*, 709–712, 1997.
- Müller, R., J.-U. Groos, D. M. McKenna, C. Brühl, J. M. Russell III, L. L. Gordley, J. P. Burrows, and A. Tuck, Chemical ozone loss in the Arctic vortex in the winter of 1995–96: HALOE measurements in conjunction with other observations, *Ann. Geophys.*, *17*, 101–114, 1999.
- Müller, R., U. Schmidt, A. Engel, D. S. McKenna, and M. H. Proffitt, The O<sub>3</sub>/N<sub>2</sub>O relationship from balloon-borne observations as a measure of Arctic ozone loss in 1991–1992, *Q. J. R. Meteorol. Soc.*, *127*, 1389–1412, 2001.
- Nash, E. R., P. A. Newman, J. E. Rosenfield, and M. R. Schoeberl, An objective determination of the polar vortex using Ertel's potential vorticity, *J. Geophys. Res.*, *101*, 9471–9478, 1996.
- Newman, P. A., et al., An overview of the SOLVE-THESE 2000 campaign, *J. Geophys. Res.*, *107*, doi:10.1029/2001JD001303, in press, 2002.
- Osterman, G. B., R. J. Salawitch, B. Sen, G. C. Toon, R. A. Stachnik, H. M. Pickett, J. J. Margitan, and D. B. Peterson, Balloon-borne measurements of stratospheric radicals and their precursors: Implications for the production and loss of ozone, *Geophys. Res. Lett.*, *24*, 1107–1110, 1997.
- Plumb, R. A., and M. K. W. Ko, Interrelationships between mixing ratios of long-lived stratospheric constituents, *J. Geophys. Res.*, *97*, 10,145–10,156, 1992.
- Plumb, R. A., D. W. Waugh, and M. P. Chipperfield, The effects of mixing on tracer relationships in the polar vortices, *J. Geophys. Res.*, *105*, 10,047–10,062, 2000.
- Popp, P. J., et al., Severe and extensive denitrification in the 1999–2000 Arctic winter stratosphere, *Geophys. Res. Lett.*, *28*, 2875–2878, 2001.
- Proffitt, M. H., and R. J. McLaughlin, Fast-response dual-beam UV-absorption ozone photometer suitable for use on stratospheric balloons, *Rev. Sci. Instrum.*, *54*, 1719–1728, 1983.
- Proffitt, M. H., et al., In situ ozone measurements within the 1987 Antarctic ozone hole from a high-altitude ER-2 aircraft, *J. Geophys. Res.*, *94*, 16,547–16,555, 1989.
- Proffitt, M. H., J. J. Margitan, K. K. Kelly, M. Loewenstein, J. R. Podolske, and K. R. Chan, Ozone loss in the Arctic polar vortex inferred from high-altitude aircraft measurements, *Nature*, *347*, 31–36, 1990.
- Proffitt, M. H., K. Aikin, J. J. Margitan, M. Loewenstein, J. R. Podolske, A. Weaver, K. R. Chan, H. Fast, and J. W. Elkins, Ozone loss inside the northern polar vortex during the 1991–92 winter, *Science*, *261*, 1150–1154, 1993.
- Ray, E. A., F. L. Moore, J. W. Elkins, G. S. Dutton, D. W. Fahey, H. Vomel, S. J. Oltmans, and K. H. Rosenlof, Transport into the Northern Hemisphere lowermost stratosphere revealed by in situ tracer measurements, *J. Geophys. Res.*, *104*, 26,565–26,580, 1999.
- Ray, E. A., F. L. Moore, J. W. Elkins, D. F. Hurst, P. A. Romashkin, G. S. Dutton, and D. W. Fahey, Descent and mixing in the 1999/2000 northern polar vortex from in situ tracer measurements, *J. Geophys. Res.*, *107*(20), doi:10.1029/2001JD000961, in press, 2002.
- Rex, M., et al., Prolonged stratospheric ozone loss in the 1995–96 Arctic winter, *Nature*, *389*, 835–838, 1997.
- Rex, M., et al., Chemical ozone loss in the Arctic winter 1994/95 as determined by the Match technique, *J. Atmos. Chem.*, *32*, 35–39, 1999a.
- Rex, M., et al., Subsidence, mixing, and denitrification of Arctic polar vortex air measured during POLARIS, *J. Geophys. Res.*, *104*, 26,611–26,623, 1999b.
- Rex, M., et al., Chemical depletion of Arctic ozone in winter 1999/2000, *J. Geophys. Res.*, *107*, 10.1029/2001JD000533, in press, 2002.
- Richard, E. C., et al., Severe chemical ozone loss inside the Arctic polar vortex during winter 1999–2000 inferred from in situ measurements, *Geophys. Res. Lett.*, *28*, 2197–2200, 2001.
- Romashkin, P. A., D. F. Hurst, J. W. Elkins, G. S. Dutton, D. W. Fahey, R. E. Dunn, F. L. Moore, R. C. Myers, and B. D. Hall, In situ measurements of long-lived trace gases in the lower stratosphere by gas chromatography, *J. Atmos. and Oceanic Technol.*, *18*, 1195–1204, 2001.
- Russell, J. M., et al., The Halogen Occultation Experiment, *J. Geophys. Res.*, *98*, 10,777–10,797, 1993.
- Salawitch, R. J., et al., Chemical loss of ozone in the Arctic polar vortex in the winter of 1991–92, *Science*, *261*, 1146–1149, 1993.
- Santee, M. L., G. L. Manney, N. J. Livesey, and J. W. Waters, UARS Microwave Limb Sounder observations of chemical processing in the 2000 Arctic late winter, *Geophys. Res. Lett.*, *27*, 3213–3216, 2000.
- Schoeberl, M. R., et al., An assessment of the ozone loss during the 1999/2000 SOLVE/THESE 2000 Arctic campaign, *J. Geophys. Res.*, *107*, 10.1029/2001JD000412, in press, 2002.
- Scott, S. G., T. P. Bui, K. R. Chan, and S. W. Bowen, The meteorological measurement system on the NASA ER-2 aircraft, *J. Atmos. Oceanic Technol.*, *7*, 525–540, 1990.
- Sen, B., G. C. Toon, G. B. Osterman, J.-F. Blavier, J. J. Margitan, R. J. Salawitch, and G. K. Yue, Measurements of reactive nitrogen in the stratosphere, *J. Geophys. Res.*, *103*, 3571–3585, 1998.
- Sen, B., et al., The budget and partitioning of stratospheric chlorine during the 1997 Arctic summer, *J. Geophys. Res.*, *104*, 26,653–26,665, 1999.
- Shindell, D. T., D. Rind, and P. Lonergan, Increased polar stratospheric ozone losses and delayed eventual recovery owing to increasing greenhouse-gas concentrations, *Nature*, *392*, 589–592, 1998.
- Sinnhuber, B. M., M. P. Chipperfield, S. Davies, J. P. Burrows, K.-U. Eichmann, M. Weber, P. von der Gathen, M. Guirlet, G. A. Cahill, A. M. Lee, and J. A. Pyle, Large loss of total ozone during the Arctic winter of 1999/2000, *Geophys. Res. Lett.*, *27*, 3473–3476, 2000.
- Toon, G. C., et al., Comparison of MkIV balloon and ER-2 aircraft measurements of atmospheric trace gases, *J. Geophys. Res.*, *104*, 26,779–26,790, 1999.
- Vömel, H., D. W. Tooney, T. Deshler, and C. Kroger, Sunset observations of ClO in the arctic polar vortex and implications for ozone loss, *Geophys. Res. Lett.*, *28*, 4183–4186, 2001.

Waugh, D. W., et al., Mixing of polar vortex air into middle latitudes as revealed by tracer-tracer scatterplots, *J. Geophys. Res.*, 102, 13,119–13,134, 1997.

World Meteorological Organization, *Scientific Assessment of Ozone Depletion: 1998, Rep. 44*, Global Ozone Res. and Monit. Proj., Geneva, 1999.

---

R. M. Bevilacqua, Naval Research Laboratory, Code 7220, Washington, DC 20375, USA. (bevilacqua@nrl.navy.mil)

T. P. Bui, NASA Ames Research Center, Mail Stop 245-5, Moffett Field, CA 94035, USA. (pbui@mail.arc.nasa.gov)

J. W. Elkins, D. F. Hurst, F. L. Moore, and P. A. Romashkin, NOAA Climate Monitoring and Diagnostics Laboratory, 325 Broadway, Mail Stop

R/CMDL1, Boulder, CO 80305, USA. (James.W.Elkins@noaa.gov; Dale.Hurst@noaa.gov; Fred.Moore@noaa.gov; Pavel.Romashkin@noaa.gov)

K. W. Hoppel, Naval Research Laboratory, Code 7227, Washington, DC 20375, USA. (Karl.Hoppel@nrl.navy.mil)

J. J. Margitan, G. B. Osterman, R. J. Salawitch, B. Sen, and G. C. Toon, Jet Propulsion Laboratory, 4800 Oak Grove Drive, Mail Stop 183-601, Pasadena, CA 91109, USA. (James.J.Margitan@jpl.nasa.gov; Gregory.B.Osterman@jpl.nasa.gov; Ross.J.Salawitch@jpl.nasa.gov; Bhaswar.Sen@jpl.nasa.gov; Geoffrey.C.Toon@jpl.nasa.gov)

E. A. Ray, NOAA Aeronomy Laboratory, 325 Broadway, Mail Stop R/AL6, Boulder, CO 80305, USA. (eray@al.noaa.gov)

M. Rex, Alfred Wegener Institute for Polar and Marine Research, P.O. Box 60 01 49, 14401 Potsdam, Germany. (mrex@awi-potsdam.de)

E. C. Richard, NOAA Aeronomy Laboratory, 325 Broadway, Mail Stop R/AL6, Boulder, CO 80303, USA. (Erik.C.Richard@noaa.gov)